Questions and observations with regard to the EIS QRA part of the planned Delimara LNG import installations (Appendix Two, Volume 7, 20 December 2013)

Reports:

1. SGS, Robert Vacari, Project for a new LNG regasification facility to be located in the Marsaxlokk Bay, QRA PRELIMINARY REPORT, Barcelona, July, 11th, 2013, Report nº.: 02-901-188098-12141 – review 0.1

2. SGS, Robert Vacari, Project for a new LNG regasification facility to be located in the Marsaxlokk Bay, QRA PRELIMINARY REPORT, Barcelona, December, 4th, 2013 Report nº.: 02-901-188098-12141 – Revision 2

The first report has been overtaken by the second one after the decisions made with respect to bidder award. So, in the following only reference is made to report 2.

LNG Hazards

The risks of LNG operations are large scale spills on water and land, rapid evaporation, cloud formation and further consequences such as flash or pool fire with strong radiant heat effects over large distance. Explosion is usually not considered as methane is a relative low-reactive hydrocarbon which does not explode in the open, but only in confined space. LNG contains however small quantities of the more reactive ethane and propane hydrocarbons. After a spill of LNG, evaporated gas is at first heavier than air but when warming up it becomes lighter and disperses easily. However, as accidents with gasoline and other hydrocarbons have shown, large masses can make a large difference and strong, destructive explosion blast effects have been observed (e.g., Buncefield, UK, Dec. 2005; Jaipur, India, Oct. 2009). A flashing flame accelerates to high velocity but details of the mechanism of the explosions are still unclear. Experiments with LNG with relative small amounts compared to a tank content of 35000 m^3 did not show any blast when ignited. Occupational hazards are asphyxiation and cold burns. Leaks in contact with normal steel cause embrittlement and loss of structural strength, which on a larger scale can impact a structure's stability. Boiling Liquid Expanding Vapor Explosion (BLEVE) in case of fire around a tank cannot be excluded but is less probable. Rapid Phase Transitions while boiling on water have so far not posed any threat. SGS considers all this. The report contains a number of statements which show the precarious character of the whole set-up/lay-out, e.g., on page 83 of 88 Conclusions, first paragraph, which highly recommends maritime risk assessments. Indeed, this can also be the summary of the comments made here: do not decide yet, but perform maritime risk assessment and look for alternatives offering more safety distance and less traffic movements. LNG accidents so far have been few, so it can be handled safely, but it is a hazardous substance and a good past record is no guarantee for the future.

1. *Accuracy of QRA studies*

   SGS performed the EIS land use risk assessment applying established methods. QRA is the best way to investigate a safety situation. However, the results have little absolute value, only relative; that is, it is useful to compare options but not more (In Annex 1 the 2000 EU study ASSURANCE is briefly summarized). Failure rates can easily be off a factor of ten or hundred. It

are probabilities which can only be validated if many of the same kind of components exist, fail in the same mode, effect of local conditions can be included and the data can be treated in a statistically sound way. For the components applied here it is not very likely that such a data base exists. And even then, if a frequency can be established as lying in a certain range with an average of once in 10,000 years it can still happen next week. If, the risk source is that close to various kinds of vulnerable receptors as is here the case safety distances are also of interest. Hence, consequence analysis as SGS has performed, provides insight in the distances hazardous effects can reach. The weakness there is that any experimental evidence with amounts as large as a tank content (35000 m^3) does not exist (the largest spill in an experiment was not even 70 m^3). The effects can be stronger or weaker than predicted. But for the time being we don't have any other information. However, to state that the maximum extension of a flashing cloud is 962 m (scenario 03.a in the revision 2 of December 2013, see also Drawing #13) is suggesting an accuracy that is not justified. Are you safe at 963 m? What is the opinion of SGS in this matter?

2. *Possible scenario of damaging the CCGT installation*
   QRAs are focused on calculating fatalities. A real large hazard in this case is however also the ingestion of leaked natural gas by the combustion devices of the power station. These become uncontrolled due to the fuel that appears all of a sudden in the air intake, even if the concentration in the air is below the explosion limit. This may lead to turbines getting out of control which may end in power failure and further escalation. If the concentration in the cloud is above the explosion limit, it may also cause strong ignition of the cloud. The mechanism of revving up a combustion engine has played a major role in several catastrophic accidents initiated by fuel leakages. SGS did only consider the hazard of a cloud being ignited at the site of the power station which would also cause heavy damage. How much margin is available in the present plan between edge of a possible cloud and air intakes (in view of drawing 13)? Has the topology of the hills surrounding the location been taken in account at a spill in case of a southern wind of low velocity?

3. *Reliability and effectiveness of protective/mitigative measures*
   The largest probability of a leak is the failure of the permanently functioning loading arm between FU and the regasification plant. What experience has been collected with the special safeguards (ERC Emergency Release Couplings) to protect against the failure of a loading hose as mentioned on page 65 of 88 about the ElectroGas proposal and in Annex C? Unreliability of a possibly sticking valve is not included. And what shall be the reliability and the effectiveness of a water curtain, more sophisticatedly called hydro-shield, in relation to scenario 03.a on page 65? Water curtains have been tested only on small scale LNG clouds and the effectiveness depends on many factors which can only be investigated by experiment. Does SGS have an answer?

4. *Cloud dispersion aspects*
   Page 38 of 88: With respect to prediction of cloud dispersion with the topological conditions mentioned (30 m high hills in all directions except West), it would make sense to make separately cloud dispersion calculations with a validated CFD code, e.g., FLACS, because the cloud dispersion models in EFFECTS (or DNV's Phast) are integral models and are unreliable for

close-in effects and interaction with obstacles and hills. Especially with heavy gas cloud and low wind this can be very important. Cloud dispersion is slowest during windless night condition and high stability, p. 36. The most favorable conditions for long stretching clouds are usually the presence of inversion layers. Please, comment.

5. *Ship-to-ship collisions*
   How will the incoming tanker manoeuver? On page 67 of 88 SGS considers in a very rudimentary way the risks of ship-ship collisions in the relative narrow and busy waterways near Marsaxlokk; why not asking this to an institute experienced in investigating ship-ship collisions and grounding? Collisions can occur between the storage tanker (floating storage unit, FSU) or incoming tank ships and departing freighters and fishing vessels, passing ships etc. Outflow of LNG on water causes rapid spreading and violent boil-off. SGS did calculate in scenarios B01.a and .b the consequence of a tank of 35000 m^3 emptying after having sustained a hole of 0.36 m^2 and reports a flash fire maximum distance of 129 and 133 m. Hightower et al. (Sandia report 2004-6258)[1], probably world's best experts on LNG risks, expect that even at very low speed and the most safe double walled tanker construction, a 90^o collision will result in a tank been pierced. (Up to 4.5 knots the tank will not be penetrated, but at 6 knots collision speed the opening in the tank becomes already 5 m^2, although there is a chance that the two ships do not separate after the collision.) An opening of 1 m^2 will be sufficient to extend the distance to the lower explosion limit to 1.5 km in case the LNG does not ignite immediately! In Boston and Rotterdam harbors stringent precautions are taken to control traffic when a tank ship arrives, but there is no permanently present FSU moored which increases the probability considerably. For a new LNG terminal in Rotterdam harbor in 2008-9 extensive maritime port safety risk assessments have been performed by the Dutch MARIN institute with long-time experience in ship collision prediction resulting in a detailed admission policy. We appreciate SGS's conclusion with respect to maritime risk assessment but what will be its comments to ship-to-ship collision consequences?

6. *Possible flame acceleration generating blast*
   It is mentioned on page 66 of 88 that as can be expected, a cloud drifting towards the regasification and further to the power station will find an ignition source. The report does not mention flame acceleration due to congestion, but that is the mechanism that makes clouds not only flashing but producing destructive blast. Pipework, fences, greenery, columns and smaller buildings provide congestion. Hence, we agree with the statement that ignition of a cloud drifted inside the plant area shall have to be prevented at all times. SGS suggested to increase the distance between the FSU and the plant. But how far is far enough? The consultant takes as the edge of the cloud the 5% lower explosion limit concentration. But pockets of gas can still be flammable below that average concentration and therefore one takes usually 60% of LEL. What is SGS' comment?

[1] Mike Hightower, Louis Gritzo, Anay Luketa-Hanlin, John Covan, Sheldon Tieszen, Gerry Wellman, Mike Irwin, Mike Kaneshige, Brian Melof, Charles Morrow, Don Ragland, *Guidance on Risk Analysis and Safety Implications of a Large Liquefied Natural Gas (LNG) Spill Over Water*, Sandia-2004-6258, December 2004

7. *Event frequency increasing human factors*
   The reports confine themselves to a generic land use planning safety aspect and do not consider the effects of operational safety. Organizational and human factors in operation and maintenance have a strong effect on the mentioned failure rates and event frequencies. The reports base themselves on Seveso II and the 2003 Amendment. These directives introduce, besides others, the safety management system and process safety performance indicator metrics. Implementing and maintaining this requires local process safety competence and in view of the complexity of the installation of relatively high expertise level. Meanwhile Seveso III is into force (2012/18/EU) emphasizing the requirement of drawing up internal Enemalta emergency plans and providing data for external community plans, while inspection/auditing requirements are further strengthened. Are there any preparations from the side of Enemalta for the safe operation of the installations, since it needs considerable time to establish this for a complex Seveso top-tier plant? Indeed, the present QRA study can only be considered as preliminary. SGS states at page 41 of 88 commenting on further hazard identification techniques as HazOp: " Experience teaches us that for highly automated and controlled processes, these techniques add no additional credible scenarios Too few details are available to make more refined analysis." Our comment is, it may not add new scenarios but it usually can increase significantly the expected frequency of existing scenarios. In case of large safety space this would not be a problem, but in view of the small distances to population, other ship traffic and industrial activities it is a problem, and a definite answer to the question is it safe enough can hardly be given. How do you comment?

8. *Operation of resupplying the FSU and of feeding the regasification unit*
   The arrival of fresh supply by LNG tanker and unloading operations are another risk source. In line with the previous point this is a rather frequent operation giving cause to leakages and spills. In itself these spills may not be large, but in case of ignition by lightning or static electricity the problem is possible escalation. The ship structures provide confinement/congestion to spilled gas. The scenarios pertain all to component failures. Why are errors in the human operations not considered? What overfilling precautions have been taken from resupply ship to FSU? How is the continuous LNG flow from FSU to regasification plant controlled? What about loss of power and emergency shutdown e.g., in case of fire? Are any fast acting valves foreseen in case of breaking loose of any of the unloading arms?

9. *Threats to the FSU due to events elsewhere in the bay area*
   Threats to the FSU due to events elsewhere are not considered. What about a hydrocarbon spill in the bay due to a collision between for example a gasoline tanker and another freight ship, causing the gasoline to ignite? What are the operations at the dolphin in the bay? The storage tanker is an easy target for malevolent action, since it is in the field of view from many land position directions. A hole in a tank of 5-7 m^2 is not that difficult to obtain. Are any security measures considered? Why are domino effects by other Seveso installations in the area not considered?

10. *Construction of the FSU*

To what specification is the FSU built? Single or double walled? How are the tanks insulated? With what materials? (Some insulating materials lose their insulating properties in case of external fire and may even themselves be combustible). At what pressures are the pressure relief valves set? How frequently can roll-overs be expected? Where is in such case the escaping vapor being led to?

11. *Stability of the FSU, its maintenance and its connection with the regasification unit*
    How is the mooring stability assured? How are the motions of the FSU relative to the fixed wall position compensated? How flexible is the connection with the on land installation and how its endurance? How will the maintenance of the FSU be handled? Is there a reserve FSU available? As there is no buffer on land, there should be a continuous supply of gas to the turbines to guarantee power supply. How will the unloading arm, the feed pump etc. behave when permanently loaded? Has there been a reliability and availability study of these parts continuously in contact with the cryogenic?

12. *Emergency planning*
    A QRA and scenario analysis serve too for emergency planning. In fact, has there already a preliminary emergency plan drafted for the whole installation? Only small fires will be extinguishable. How will alarming and evacuation of workers and near-by population be organized? Emergency response will have also to come from the community, short response time is essential, how will the local councils cater for that?

13. *Need for technical details to appreciate the safety situation*
    We understand that so far few technical details on the installation are provided. However the devil for safety is often in the detail. So, when can more information be expected?

14. *Some detail questions:*
    Page 19 of 88: What purpose serves the propane system? P. 37: Releases on the jetty: 'pipeline from ship to storage tank'. What tank? There is no LNG tank on land, or is there?

N.B. There is an extensive Annex D on acceptance criteria, which can also trigger quite a few questions and comments, but I assume Malta does not have quantitative risk criteria cast in law and acceptance will be on adequacy of design, site positioning, lay-out and risk reducing measures taken including the ALARP (as low as reasonably practical). Hence, this annex may not be relevant at this time. SGS does mention in the annex US Department of Energy but not the US FERC acceptance regulation for LNG (exclusion zoning), which is on radiant heat threshold (5 kW/m^2) and vapor concentration (50% LEL) limits.

St Julian's, 13 January 2014

Hans J. Pasman

ANNEX 1 Accuracy of QRA's, Project ASSURANCE

Results of a QRA-calculation should be considered with caution, because uncertainty is larger than an order of magnitude. Twice at the European Union level, a benchmark exercise was organized to evaluate risk analysis models; the second EU project ASSURANCE is most relevant.

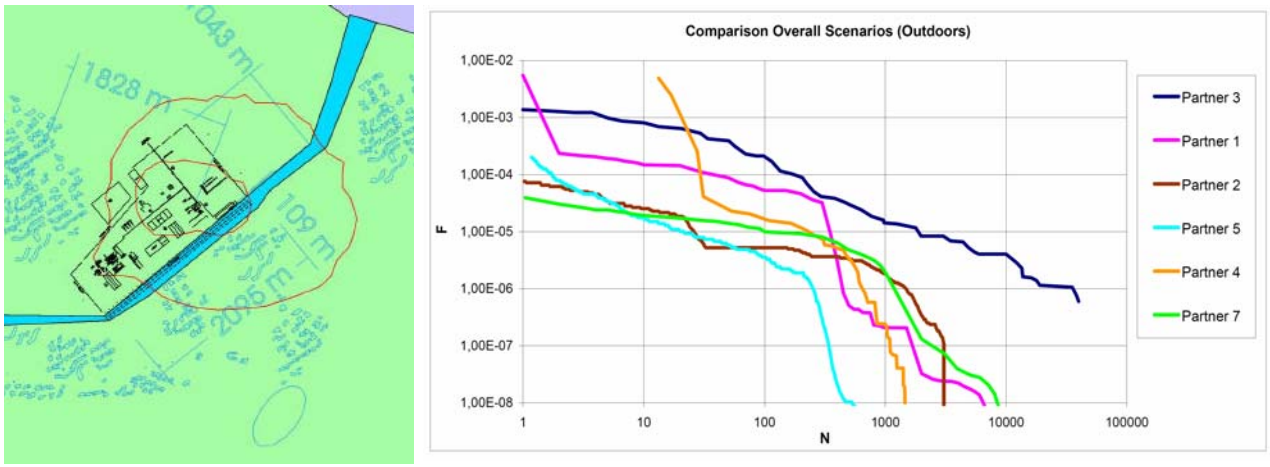

Figure 1. Results of EU Benchmark exercise ASSURANCE 2002 by Lauridsen et al.[2]. *Left:* Maximum and minimum 10^{-5} /yr risk contour found in the analysis: since the large one lies for a major part outside the plant's premises, this result will present a dilemma to decision makers. *Right:* Societal risk results expressed in *F-N* curves differing by two orders of magnitude.

Table: Contributing factors to the variance in risk analysis results, according to Lauridsen et al.

Uncertainty Factor	**Importance**
Differences in the qualitative analysis	**
Factors relating to frequency assessment:	
Frequency assessments of pipeline failures	***
Frequency assessments of loading arm failures	****
Frequency assessments of pressurized tank failures	****
Frequency assessments of cryogenic tank failures	***
Factors relating to consequence assessment:	
Definition of the scenario	*****
Modeling of release rate from long pipeline	***
Modeling of release rate from short pipeline	*
Release time (i.e. operator or shut-down system reaction time)	***
Choice of light, neutral, or heavy gas model for dispersion	****
Differences in dispersion calculation codes	***
"Analyst conservatism" or judgment	***

[2] Kurt Lauridsen, Igor Kozine, Frank Markert, Aniello Amendola, Michalis Christou, Monica Fiori, Assessment of Uncertainties in Risk Analysis of Chemical Establishments, The ASSURANCE project Final summary report, Risø National Laboratory, Roskilde, Denmark, May 2002, 52 p., http://www.risoe.dk/rispubl/sys/syspdf/ris-r-1344.pdf.

This risk analysis project, published by Lauridsen et al., was performed by seven all highly experienced teams on an ammonia storage plant with loading/unloading operations. For this exercise, the plant was virtually located in Denmark. The teams were asked this time to perform a complete risk analysis so that all variability factors were included. Although the spread in results had decreased compared to a ten-year earlier exercise in which only the dispersion model was a parameter, the root problems of spread had not been solved.

Individual risk contours (10^{-5} per year, see Figure 1, *left*) differed by at least a factor of 3 in radius, which is a very large spread in area. The two extremes, smallest and largest, result in either license granted or denied, because the latter contour runs outside the plant premises across parts of a nearby township.

Group risk (*F-N* curves, see Figure 1, *right*) differed by over 2 orders of magnitude.

The relative importance of various contributing sources of uncertainty is summarized in the table. The largest contribution to uncertainty appeared to be the variety in the scenario definition, where analyst judgment and selection of release modes leads to large differences in effects. Next, large contributors are failure rate (frequency assessment) values and the choice of dispersion model.

Further comments on the QRA of LNG storage and handling in Marsaxlokk Harbour

1. The QRA as performed by SGS is not only preliminary in the sense that it lacks precise data on the construction and sub-systems of storage ship and regasification installation, but it is also seriously incomplete because it does not contain a risk consideration of ship-to-ship collisions and other maritime risks, while the pool formation on water from a leak in one of the 35,000 m^3 tanks is treated very unsatisfactorily. Regrettably, the latter I became aware of after the public meeting, because these scenarios present consequences on the largest distances.
2. In fact, the permanent presence of at maximum 130,000 m^3 LNG in a floating storage unit and the temporary presence of a supply ship with the same amount form a threat to the power station, the container harbour, fishing ships, lives and health of people the vicinity. LNG stored in a water environment allowing unbounded pool formation is inherently much more unsafe than stored on land in a bunded park with double walled tanks.
3. In scenarios B01a and b of a tank wall penetration (gas tanker – release on water) Mr. Roberto Vaccari assumed a maximum pool spread area of 10,000 m^2. This assumption was based on three Dutch references ([21], [22], [25]), all known to me. Apart from the fact that I couldn't find the 10,000 m^2 in the reports, nor any statements where it could be derived from, but it may be implied somewhere, I don't believe it is a fixed value. The area is determined by the leak rate, the spreading rate and the evaporation rate, and in general it will be larger with a larger rate of outflow. Calculation is complex and difficult. Fay (MIT, US) and Webber (HSL, UK) present equations, but CFD would be better. Not all physical properties of LNG are well known. Validation is not well possible, while there are only results of a few, old, small amount tests available.
4. A recent paper in Process Safety Progress (attached) by a renowned American specialist expert (Mike Hightower, at Sandia) in this particular LNG risk aspect (with huge computer power at his disposal and funding by the US Senate) mentions the following distances depending on whether the cloud is ignited and forms a burning pool, or whether all LNG evaporates and a cloud drifts away:

   1 m^2 hole, burning pool, Ø = 148 m, injury threshold population (5 kW/m^2) = 554 m
   2 209 m 784 m
   5 405 m 1579 m
   1 , dispersion , 148 m, distance to explosion limit 1536 m
   2 209 m, 1710 m
   5 405 m, 2450 m.
5. The larger the leak hole the shorter the spill time (40 minutes at 1 m^2 to 8 minutes at 5 m^2) The paper does not specify all weather conditions as these will have an effect, but it is clear that the distances in the SGS report of 129, 133 and 138 m of the B01 scenarios (page 65 of 88 in revision 2) are a severe underestimate. The probability of such a hole depends much on the conclusions of a maritime risk analysis.
6. About the dispersion model applied in the TNO Riskcurves software can be mentioned that it is a so-called integral model (2nd generation) taking account of heavy gases such as chlorine.

How it behaves with a gas as LNG that is initially heavy, slowly warms up and becomes lighter than air, I don't know. It is certainly not suited for hilly terrain, buildings and *low* wind speeds. The only type of models that can calculate this kind of situations is the 3rd generation Computational Fluid Dynamic (CFD) type. The only CFD model that is rather recently validated and approved by the US authorities, is the Norwegian one I already mentioned and is called FLACS. Attached is the 2010 paper. That the US FERC (Federal Energy Regulatory Commission) approved is important, because in the US the safe distance is dependent on the dispersion and dilution till half the lower explosion limit, which is 2.5%.

7. Low wind speeds, below 2 m/s, create the most hazardous conditions. Figure 4 shows e.g., test MS27 (Maplin Sands near Thames estuary UK in 1980) at 5.5 m/s wind speed a distance to till 2.5% LNG of about 350 m. The release rate was 23 kg/s. Mr. Vaccari mentions for scenario B01, 732 and 856 kg/s, which I think is not too high, only about 1 m^3 per second!!
8. Failure probabilities for the components such as hoses, loading arms, and others are guesses. One cannot rely on it. There is some data collected in the US I expect, but I still have to see a sound data base on LNG components. So, risk figures are rather uncertain.
9. The used model and the risk criteria (individual risk and to a lesser extent societal risk) have to be considered in the Dutch context of Land Use Planning against the background of compromises government-industry. If people really get upset, as in a recent case of carbon dioxide sequestration pilot test at Barendrecht near Rotterdam, the government backed off, although the risk curves were much below criteria. Also there, many uncertainties played a role.

Ruurlo, Nl, 29-01-2014 / H.J. Pasman

Safety Implications of a Large LNG Tanker Spill over Water

Michael Hightower, Louis Gritzo, and Anay Luketa-Hanlin
Sandia National Laboratories, P.O. Box 5800 Albuquerque, NM 87185; mmhight@sandia.gov (for correspondence)
DOI 10.1002/prs.10089

Published online 12 July 2005 in Wiley InterScience (www.interscience.wiley.com).

The increasing demand for natural gas in the United States could significantly increase the number and frequency of marine LNG (liquefied natural gas) imports. Although many studies have been conducted to assess the consequences and risks of potential LNG spills, the increasing importance of LNG imports suggests that consistent methods and approaches be identified and implemented to help ensure protection of public safety and property from a potential LNG spill.

For that reason, the U.S. Department of Energy (DOE), Office of Fossil Energy, requested that Sandia National Laboratories (Sandia) develop guidance on a risk-based analysis approach to assess and quantify potential threats to an LNG ship, the potential hazards and consequences of a large spill from an LNG ship, and review prevention and mitigation strategies that could be implemented to reduce both the potential and the risks of an LNG spill over water.

Specifically, DOE requested:

- An in-depth literature search of the experimental and technical studies associated with evaluating the safety and hazards of an LNG spill from an LNG ship
- A detailed review of four recent spill modeling studies related to the safety implications of a large-scale LNG spill over water
- Evaluation of the potential for breaching an LNG ship cargo tank, both accidentally and intentionally, identification of the potential for such breaches and the potential size of an LNG spill for each breach scenario, and an assessment of the potential range of hazards involved in an LNG spill
- Development of guidance on the use of modern, performance-based, risk management approaches to analyze and manage the threats, hazards, and consequences of an LNG spill over water to reduce the overall risks of an LNG spill to levels that are protective of public safety and property.

This paper provides an overview of the conclusions and recommendations from that study. © 2005 American Institute of Chemical Engineers Process Saf Prog 24: 168–174, 2005

BACKGROUND

To support this effort, Sandia National Laboratories (Sandia) worked with the U.S. Department of Energy (DOE), the U.S. Coast Guard, LNG industry and ship management agencies, LNG shipping consultants, and government intelligence agencies to collect background information on ship and liquefied natural gas (LNG) cargo tank designs, accident and threat scenarios, and standard LNG ship safety and risk management operations. The information gathered was used to develop accidental and intentional LNG cargo tank breach scenarios, for modeling of potential spill hazards, and as the basis for analysis to determine the extent and severity of LNG spill consequences. Based on analysis of the modeling results, three consequence-based hazard zones were identified. In addition, risk reduction and mitigation techniques were identified to reduce impacts on public safety and property.

The results from the Sandia study were reviewed by an external peer review panel and made available to the public in a recent Sandia report "Guidance on Risk Analysis and Safety Implications of a Large Liquefied Natural Gas (LNG) Spill Over Water" [1]. The overall role of the report was to provide communities and agencies with suggestions and guidance on how to consider various issues, including terminal location and site conditions, operational conditions, environmental effects, and safety and security issues and measures to achieve appropriate levels of protection of public safety and property for LNG imports.

*This article was prepared as an account of work sponsored by an agency of the United States government.

Several analysis techniques are available to help identify the possible hazards to the public from activities that occur in modern society such as hazardous material manufacturing, transportation, or use. These include vulnerability analyses, safety analyses, and consequence analyses. These techniques have become elements of modern, performance-based risk analysis and risk management approaches. In modern risk analysis, the risks associated with an event are commonly defined as a function of the following four elements:

- The probability of an event—such as an LNG cargo tank breach and spill
- The hazards associated with the event—such as thermal radiation from a fire arising from an LNG spill
- The consequences of the event—such as the thermal damage from a fire
- The effectiveness of systems for preventing the event or for mitigating the hazards and consequences—such as any safety/security systems

Therefore, discussions of the safety issues of hazardous operations, such as LNG imports and transportation, should include not only discussions of vulnerability and safety analyses, but also risk management considerations that can help reduce the possibility or impacts of an event and improve the overall safety and protection of the public and property from the event. In the sections below we discuss the results of the vulnerability and safety analyses conducted, as well as discuss risk and safety management options that should be considered to improve overall public safety from possible spills during LNG import operations.

LNG Breach, Spill, and Hazard Analyses

Currently, the potential for an LNG cargo tank breach, whether accidental or intentional, the dynamics and dispersion of a large spill, and the hazards of such a spill are not fully understood, for two primary reasons. First, the combination of current LNG ship designs and safety management practices for LNG transportation have reduced LNG accidents to the extent that there is little historical or empirical information on the consequences of breaches or large spills. Second, current experimental data on LNG spill dynamics and its dispersion over water address spill volumes that are more than a factor of 100 smaller than spill sizes currently being postulated for some intentional events. Variations in site conditions, LNG ship designs, and environmental conditions further complicate hazard predictions.

The lack of large-scale experimental data forces analysts to make many assumptions and simplifications in calculating the breach of an LNG cargo tank, the resulting spill dispersion, and associated thermal hazards. For example, an evaluation of four recent LNG spill studies showed significant differences in thermal hazard estimates as the result of the differences in assumptions and modeling approaches used in each analysis [2–5].

Although current spill assessment and modeling techniques and validation of models against large-scale LNG spill data have limitations, the guidance provided is applicable to performance-based hazard and risk management approaches. Such approaches can be used in conjunction with existing spill and hazard analysis techniques, and safety and security methods, to assess and reduce the risks to both public safety and property caused by an LNG spill over water. Guidance is provided on the use of existing analysis techniques applied to site-specific conditions for increasing confidence in the management of hazards and risks. As additional LNG spill data are obtained and hazard analysis models are improved, they can be incorporated into future risk analysis guidance.

LNG Cargo Tank Breach Analysis

Based on available information, a range of historically credible and potential accidental and intentional events was identified that could cause an LNG cargo tank breach and spill. Modern finite-element modeling and explosive shock physics modeling were used to estimate a range of breach sizes for credible accidental and intentional LNG spill events, respectively [1].

From these analyses, the sizes of LNG cargo tank breaches for accidents were estimated to be <2 m^2 (1.6 m diameter). For intentional events, the size of the hole depends on its location on the ship and the source of the threat. Intentional breaches were estimated at <2 m^2 to approximately 12 m^2 ($<$1.6 to 4 m diameter) with nominal sizes of about 5–7 m^2 (2.5–3.0 m diameter). The breach sizes estimated can lead to large LNG spills.

Using structural fracture mechanics analyses, we also evaluated the potential for cryogenic damage to the LNG ship and other LNG cargo tanks. Based on these analyses, the potential for cryogenic damage to the ship cannot be ruled out, especially for large spills. The degree and severity of damage depends on the size and location of the breach. Sandia considered cryogenic damage to the ship's structure and concluded that releases from no more than two or three tanks at a time would be involved in a spill that occurs as the result of any single incident. This cascading release of LNG was analyzed and is not expected to significantly increase the overall fire size or hazard ranges, although the expected fire duration will increase. Hazard analysis and risk prevention and mitigation strategies should consider this in assessing public safety and damage to property.

Spill and Dispersion Analyses

The variability in existing LNG spill and dispersion/thermal hazard modeling approaches is explained by physical limitations in the models and the lack of validation with large-scale spill data. Obtaining experimental data for large LNG spills over water would provide needed validation and help reduce modeling uncertainty. Because extrapolation of existing models will be necessary for analysis of potentially large spills, models should be used that invoke as much fundamental physics as possible. Based on the evaluations presented in the report, several types of models currently exist to assess hazards. Models should be used only where they are appropriate and understood to ensure

Table 1. Models for improved analysis of an LNG spill in high-hazard areas.

Application	Improved Modeling Approaches
Breach analysis	Finite-element codes for modeling accidental ship collisions and shock physics codes for modeling intentional breaches.
Tank emptying	Modified orifice model that includes the potential for LNG leakage between hulls.
Structural damage modeling	Coupled spill leakage, fluid flow, and fracture mechanics codes for modeling ship structural damage and damage to LNG cargo tanks.
Spreading	CFD codes for modeling spread of cryogenic liquids on water such as FLOW-3D or STORM/CFD2001.
Dispersion	CFD codes for modeling dispersion of dense gases such as FEM3C, FLUENT, CFX, FDS, or Fuego.
Fire	FDS CFD codes for modeling fire phenomena, including combustion, soot formation, and radiative heat transfer such as FLACS, CFX, FDS, Phoenics, Kameleon, Vulcan, or Fuego.

that the results increase confidence in the analysis of the hazards and risks to public safety and property.

In higher hazard zones, where analysis reveals that potential impacts on public safety and property could be high and where interactions from a spill are close enough to shore where interaction with terrain or structures can occur, modern, computational fluid dynamics (CFD) models, as listed in Table 1, can be used to improve analysis of site-specific hazards, consequences, and risks. Use of these models is suggested because many of the simpler models have limitations that can cause greater uncertainties in calculating liquid spread, vapor dispersion, and fire hazards. CFD models have their own limitations and must be validated before use. Further refinement of CFD models will continue to improve the degree of accuracy and reliability for consequence modeling.

Although these studies provide insight into appropriate models to use, additional factors should be considered in applying models to a specific problem. These include model documentation and support, assumptions and limitations, comparison and validation with data, change control and upgrade information, user support, appropriate modeling of the physics of a spill, modeling of the influence of environmental conditions, spill and fire dynamics, and model peer review.

Hazards Analysis and Public Safety Impacts

Current LNG spill and dispersion modeling and analysis techniques have limitations. In addition, variations exist in location-specific conditions that influence dispersion, such as terrain, weather conditions, waves, currents, and the presence of obstacles. Therefore, it is sensible to provide guidance on the general range of hazards for potential spills rather than suggest a specific, maximum hazard guideline.

To assess the general magnitude of expected hazard levels, a limited sensitivity analysis was performed using simplified models for a range of spill volumes. The spill volumes were based on potential breaches from credible accidental and intentional threats and approximated about 12,500 m^3 for each tank breached [1]. Although not conducted for a specific site, the analyses provide examples of general considerations for hazards and risks. The general results are presented in Table 2 for a set of possible breaches and an ensuing fire, and Table 3 for a spill without ignition and vapor cloud dispersal in a wind speed of 2.33 m/s at 10 m above the ground and in an F class atmospheric stability.

The values used for burn rate and surface emissive power are based on the nominal values measured from large-scale LNG spill and fire test data over water [1]. In Table 2, the burn rate defines the mass of LNG burned per square meter of pool area. Most of the events considered should provide an ignition source and the likelihood of a large unignited release of LNG is unlikely. A vapor cloud dispersion of LNG will also have a tendency to create a more linear hazard zone rather than a generally circular hazard zone expected from an LNG spill fire. The 37.5 and 5 kW/m^2 values shown in Table 2 are thermal flux values commonly recognized for defining hazard distances for LNG [6]. The value 37.5 kW/m^2 is a level suggesting severe structural damage and major injuries if expected for over 10 min. The value 5 kW/m^2 is a level suggesting second-degree skin burns on exposed skin if expected for periods of over about 20 s, and is the value suggested as the protection standard for people in open spaces. These values were considered as defining the bounds between high-, medium-, and low-hazard zones from a fire.

From the assessment conducted, thermal hazards will occur predominantly within 1600 m of an LNG ship spill, with the highest hazards generally in the near field (approximately 250–500 m of a spill). Although thermal hazards can exist beyond 1600 m, they are generally lower in most cases.

The general hazard zones and safety guidance identified from the study are as follows:

- The pool sizes for credible spills could range from generally 150 m in diameter for a small, accidental spill to several hundred meters for a large, intentional spill. Therefore, high thermal hazards from a fire are expected to occur within approximately 250–500 m from the origin of the spill, depending on the size of the spill. Major injuries and significant structural damage are possible in this zone. The extent of the hazards will depend on the spill size and dispersion from wind, waves, and currents. People, major commercial/industrial areas,

Table 2. Potential thermal hazard distances for several possible breaching events.

Hole Size (m^2)	Tanks Breached	Discharge Coefficient	Burn Rate (m/s)	Surface Emissive Power (kW/m^2)	Pool Diameter (m)	Burn Time (min)	Distance to 37.5 kW/m^2 (m)	Distance to 5 kW/m^2 (m)
Accidental Events								
1	1	0.6	3×10^{-4}	220	148	40	177	554
2	1	0.6	3×10^{-4}	220	209	20	250	784
Intentional Events								
5	3	0.6	3×10^{-4}	220	572	8.1	630	2118
5*	1	0.6	3×10^{-4}	220	330	8.1	391	1305
5	1	0.9	3×10^{-4}	220	405	5.4	478	1579
5	1	0.6	8×10^{-4}	220	202	8.1	253	810
5	1	0.6	2×10^{-4}	220	395	8.1	454	1538
5	1	0.6	3×10^{-4}	175	330	8.1	314	1156
5	1	0.6	3×10^{-4}	350	330	8.1	529	1652
12	1	0.6	3×10^{-4}	220	512	3.4	602	1920

*Nominal case.

Table 3. Potential lower flammability limit (LFL) distances for possible vapor dispersions.

Hole Size (m^2)	Tanks Breached	Pool Diameter (m)	Spill Duration (min)	Distance to LFL (m)
Accidental Events				
1	1	148	40	1536
2	1	209	20	1710
Intentional Events				
5	1	405	8.1	2450
5	3	572	8.1	3614

or other critical infrastructure elements, such as chemical plants, refineries, bridges or tunnels, or national icons located within portions of this zone could be seriously affected.

- Hazards and thermal impacts transition to lower levels with increasing distance from the origin of the spill. Some potential for injuries and property damage can still occur in portions of this zone, although this will vary based on spill size, distance from the spill, and site-specific conditions. For small spills, the hazards transition quickly to lower hazard levels.
- Beyond approximately 750 m for small accidental spills and 1600 m for large spills, the impacts on public safety should generally be low for most potential spills. Hazards will vary; but minor injuries and minor property damage are most likely at these distances. Increased injuries and property damage would be possible if vapor dispersion occurred and a vapor cloud was not ignited until after reaching this distance.

Table 4 summarizes the results on expected hazard levels for several types of accidental and intentional spills. Although the analyses included evaluations of the size and number of breaches, spill rate and discharge coefficient, burn rate, surface emissive power, and transmissivity, site-specific environmental conditions such as wind speed, direction, waves, and currents were not specifically considered. Therefore, the distances to each of the different hazard zones are provided as guidance and will vary depending on site-specific conditions and location. The top part of Table 4 identifies the estimated hazard zones for public safety from potential accidents, where spills are generally small, whereas the bottom part of Table 4 identifies the estimated hazard zones for public safety from intentional LNG spills, which can be larger if spill prevention and mitigation approaches are not effectively implemented.

Many of the hazard zones identified in Table 4 are based on thermal hazards from a pool fire, given that many of the events will provide ignition sources such that a fire is likely to occur immediately. In some cases, the potential exists for a vapor cloud to be created without being ignited. A vapor cloud from an LNG spill could extend to 2500 m for nominal conditions, if an ignition source is not available. The potential thermal hazards within a vapor cloud could be high. Because vapor cloud dispersion is highly influenced by atmospheric conditions, hazards from this type of event will be very site specific. In addition, latent or indirect effects, such as additional damage that could be caused by a damaged infrastructure (such as a refinery or power plant), were not directly assessed. These types of issues and concerns are site specific and should be included as part of the overall risk management process.

RISK MANAGEMENT FOR LNG OPERATIONS OVER WATER

Risks and hazards from a potential LNG spill over water could be reduced through a combination of approaches, including (1) reducing the potential for a spill; (2) reducing the consequences of a spill; or (3)

Table 4. Guidance for impacts on public safety from LNG breaches and spills.

Event	Potential Ship Damage and Spill	Potential Hazard	Potential Impact on Public Safety*		
			High	Medium	Low
Collisions: Low speed	Minor ship damage, no spill	Minor ship damage	None	None	None
Collisions: High speed	LNG cargo tank breach and small to medium spill	Damage to ship and small fire	~250 m	~250–750 m	>750 m
Grounding: <3 m high object	Minor ship damage, no breach	Minor ship damage	None	None	None
Intentional breach	Intentional breach and medium to large spill	Damage to ship and large fire	~500 m	~500–1600 m	>1600 m
	Intentional, large release of LNG	Damage to ship and large fire	~500 m	~500–1600 m	>1600 m
		Vapor cloud dispersion with late ignition	~500 m	>1600 m	>2000 m

*Distance to spill origin, varies according to site: Low.-minor injuries and minor property damage; Medium.-potential for injuries and property damage; High.-major injuries and significant damage to property.

improving LNG transportation safety equipment, security, or operations to prevent or mitigate a spill.

For example, a number of international and U.S. safety and design standards have been developed for LNG ships to prevent or mitigate an accidental LNG spill over water. These standards are designed to prevent groundings, collisions, and steering or propulsion failures. They include traffic control, safety zones around the vessel while in transit within a port, escort by Coast Guard vessels, and coordination with local law enforcement and public safety agencies. These efforts have been exemplary, and in over 40 years of LNG marine transport operations there have been no major accidents or safety problems either in port or on the high seas [7]. In addition, since September 11, 2001, additional security measures have been implemented to reduce the potential for intentional LNG spills over water. They include earlier notice of a ship's arrival (from 24 to 96 h), investigation of crew backgrounds, at-sea boardings of LNG ships, special security sweeps, and positive control of an LNG ship during port transit.

Proactive risk management approaches can help reduce both the potential and hazards of such events. These include

- Improvements in ship and terminal safety/security systems, including improved surveillance, tank and insulation upgrades, and tanker standoff protection systems
- Modifications and improvements in LNG tanker escorts, extension of vessel movement control zones, and safety operations near ports and terminals
- Improved surveillance and searches of tugs, ship crews, and vessels
- Redundant or offshore mooring and offloading systems
- Improved emergency response systems to reduce fire and dispersion hazards and improved emergency response coordination and communication

Risk prevention and mitigation techniques can be important tools in reducing both the potential for and the hazards of a spill, especially in zones where the potential impact on public safety and property can be high. However, what might be applicable for effective risk reduction in one location might not be appropriate at another. Table 5 provides examples of how implementation of different strategies, alone or in combination, can be used to reduce certain threats, mitigate consequences of a spill, or reduce hazard analysis uncertainties.

Risk identification and risk management processes should be conducted in cooperation with appropriate stakeholders, including public safety officials and elected public officials. Considerations should include site-specific conditions, available intelligence, threat assessments, safety and security operations, and available resources. This approach should be based on performance and include identification of site-specific hazards and risks and protection needs.

Based on the safety and risk mitigation and prevention evaluations, the following guidance is provided to assist risk management professionals, emergency management and public safety officials, port security officials, and other appropriate stakeholders in developing and implementing appropriate safety and risk management strategies and processes for LNG import operations. For both accidental and intentional spills:

- Use effective security and protection operations that include enhanced interdiction, detection, delay procedures, risk management procedures, and

Table 5. Representative options for LNG spill risk reduction.

Impact on Public Safety	Reduction in Event Potential (Prevention)	Improve System Security and Safety (Mitigation)	Improved Hazard Analysis (Reduce Analytical Uncertainties)	Resultant Risk Reduction
High and medium	• Early offshore interdiction • Ship inspection • Control of ship, tug, and other vessel escorts • Vessel movement control zones (safety/security zones) • One-way traffic • LNG offloading system security interlocks	• Harbor pilots • Ship and terminal safety and security upgrades • Expanded emergency response and fire fighting to address fires, vapor clouds, and damaged vessels	• Use of validated CFD models for LNG spill and thermal consequence analysis for site specific conditions • Use of CFD and structural dynamic models for spill/structure interactions	Combination of approaches to reduce risks to acceptable levels
Low	Use of existing best risk management practices on traffic control, monitoring, and safety zones	Use of existing best risk mitigation practices to ensure risks remain low	Use of appropriate models to ensure hazards are low for site-specific conditions	Combination of approaches to ensure risks are maintained at acceptable levels

coordinated emergency response measures, to reduce the risks from a possible breaching event.
- Implement risk management strategies based on site-specific conditions and the expected impact of a spill on public safety and property. Less intensive strategies would often be sufficient in areas where the impacts of a spill are low.
- Where analysis reveals that potential impacts on public safety and property could be high and where a spill could interact with terrain or structures, modern, validated (CFD) models can be used to improve analysis of site-specific hazards.

SAFETY ANALYSIS AND RISK MANAGEMENT CONCLUSIONS

The potential for damage that could result from accidents or intentional events was evaluated. Although hazard distances and levels will vary based on site-specific conditions, a summary of the safety analysis conclusions and risk management guidance is presented below.

General Conclusions

1. The most significant impacts to public safety and property exist within approximately 500 m of a spill, with much lower impacts at distances beyond 1600 m, even for very large spills.
2. Under certain conditions, it is possible that multiple LNG cargo tanks could be breached, either as a result of the breaching event itself, as a consequence of LNG-induced cryogenic damage to nearby tanks, or from fire-induced structural damage to the vessel.
3. Multiple breach and cascading LNG cargo tank damage scenarios were analyzed. Although possible under certain conditions, they are likely to involve no more than two to three cargo tanks at any one time. These conditions will not greatly change the hazard ranges noted in General Conclusion 1, but will increase expected fire duration.

Accidental Breach Scenario Conclusions

1. Accidental LNG cargo tank damage scenarios exist that could potentially cause an effective breach area of 0.5 to 1.5 m^2.
2. Because of existing design and equipment requirements for LNG carriers, and the implementation of navigational safety measures such as traffic management schemes and safety zones, the risk from accidents is generally low.
3. The most significant impacts to public safety and property from an accidental spill exist within approximately 250 m of a spill, with lower impacts at distances beyond approximately 750 m from a spill.

Intentional Breach Scenario Conclusions

1. Several credible, intentional LNG cargo tank damage scenarios were identified that could initiate a breach of between 2 m^2 (1.6 m diameter) to approximately 12 m^2 (4 m diameter), with a probable nominal size of 5–7 m^2 (2.5–3.0 m diameter).
2. Most of the intentional damage scenarios identified produce an ignition source and an LNG fire is very likely to occur.

3. Some intentional damage scenarios could result in vapor cloud dispersion, with delayed ignition and a fire.
4. Several intentional damage scenarios could affect the structural integrity of the vessel or other LNG cargo tanks as a result of ignition of LNG vapor trapped within the vessel. Although possible under certain conditions, these scenarios are likely to involve no more than two to three cargo tanks at any one time.
5. Rapid phase transitions (RPTs) are possible for large spills. Effects will be localized near the spill source and should not cause extensive structural damage.
6. The potential damage from spills to critical infrastructure elements such as bridges, tunnels, industrial/commercial centers, LNG unloading terminals and platforms, harbors, or populated areas can be significant in high-hazard zones.
7. In general, the most significant impacts on public safety and property from an intentional spill exist within approximately 500 m of a spill, with lower impacts at distances beyond approximately 1600 m from a spill, even for very large spills.

Guidance on Risk Management for LNG Spills

Zone 1. These are areas in which LNG shipments transit narrow harbors or channels, pass under major bridges or over tunnels, or come within approximately 250 m for accidental spills or 500 m for intentional spills, of people and major infrastructure elements, such as military facilities, population and commercial centers, or national icons. Within this zone, the risk and consequences of an LNG spill could be significant and have severe negative impacts. Thermal radiation poses a severe public safety and property hazard, and can damage or significantly disrupt critical infrastructure located in this area.

Risk management strategies for LNG operations should address both vapor dispersion and fire hazards. Therefore, the most rigorous deterrent measures, such as vessel security zones, waterway traffic management, and establishment of positive control over vessels, are options to be considered as elements of the risk management process. Coordination among all port security stakeholders is essential. Incident management and emergency response measures should be carefully evaluated to ensure adequate resources (that is, firefighting, salvage, etc.) are available for consequence and risk mitigation.

Zone 2. These are areas in which LNG shipments and deliveries occur in broader channels or large outer harbors, or within approximately 250–750 m for accidental spills or 500–1500 m for intentional spills, of major critical infrastructure elements such as population or commercial centers. Thermal radiation transitions to less severe hazard levels to public safety and property. Within Zone 2, the consequences of an LNG spill are reduced and risk reduction and mitigation approaches and strategies can be less extensive.

Within Zone 2, the consequences of an LNG spill are reduced and risk reduction and mitigation approaches and strategies can be less extensive. In this zone, risk management strategies for LNG operations should focus on approaches dealing with both vapor dispersion and fire hazards. The strategies should include incident management and emergency response measures such as ensuring areas of refuge (such as enclosed areas, buildings) are available, development of community warning signals, and community education programs to ensure persons know what precautions to take.

Zone 3. This zone covers LNG shipments and deliveries that occur more than approximately 750 m for accidental spills or 1600 m for intentional spills from major infrastructures, population/commercial centers, or in large bays or open water, where the risks and consequences to people and property of an LNG spill over water are minimal. Thermal radiation poses minimal risks to public safety and property.

Within Zone 3, risk reduction and mitigation strategies can be significantly less complicated or extensive. Risk management strategies should concentrate on incident management and emergency response measures that are focused on dealing with vapor cloud dispersion. Measures should ensure areas of refuge are available, and community education programs should be implemented to ensure that persons know what to do in the unlikely event of a vapor cloud.

LITERATURE CITED

1. M. Hightower, L. Gritzo, A. Luketa-Hanlin, J. Covam, S. Tieszen, G. Wellman, M. Irwin, M. Kaneshig, B. Melof, C. Morrow, D. Ragland, Guidance on risk analysis and safety implications of a large liquefied natural gas (LNG) spill over water, SAND2004-6258, Sandia National Laboratories, Albuquerque, NM, December 2004.
2. W. Lehr and D. Simecek-Beatty, Comparison of hypothetical LNG and fuel oil fires on water, Draft report by the National Oceanic and Atmospheric Administration (NOAA), Office of Response and Restoration, Seattle, WA, 2003.
3. J.A. Fay, Model of spills and fires from LNG and oil tankers, J Hazard Mater B96 (2003), 171–188.
4. Quest Consultants, Inc., Modeling LNG spills in Boston Harbor, Letter from Quest Consultants to U.S. Department of Energy (DOE) (October 2, 2001); Letter from Quest Consultants to DOE (October 3, 2001); and Letter from Quest Consultants to DOE (November 17, 2003), Quest Consultants, Norman, OK.
5. LNG Health and Safety Committee of the Disaster Council of the City of Vallejo, CA, Liquefied natural gas in Vallejo: Health and safety issues, January 2003.
6. National Fire Protection Association (NFPA), Standard for the protection, storage, and handling of liquefied natural gas, NFPA 59A, NFPA, Quincy, MA, 2001.
7. R.M. Pitblado, J. Baik, G. Hughes, C. Ferro, and S. Shaw, Consequences of LNG marine incidents, Proc Center for Chemical Process Safety (CCPS) Conf, Orlando, FL, June 30–July 2, 2004.

Journal of Loss Prevention in the Process Industries 23 (2010) 857–877

Contents lists available at ScienceDirect

Journal of Loss Prevention in the Process Industries

journal homepage: www.elsevier.com/locate/jlp

Validation of FLACS against experimental data sets from the model evaluation database for LNG vapor dispersion

Olav R. Hansen, Filippo Gavelli*, Mathieu Ichard, Scott G. Davis

GexCon US, 7735 Old Georgetown Rd., Suite 1010, Bethesda, MD 20814, USA

ARTICLE INFO

Article history:
Received 2 March 2010
Received in revised form
1 August 2010
Accepted 2 August 2010

Keywords:
LNG
Dense gas dispersion
Consequence modeling
CFD
FLACS

ABSTRACT

The siting of facilities handling liquefied natural gas (LNG), whether for liquefaction, storage or regasification purposes, requires the hazards from potential releases to be evaluated. One of the consequences of an LNG release is the creation of a flammable vapor cloud, that may be pushed beyond the facility boundaries by the wind and thus present a hazard to the public. Therefore, numerical models are required to determine the footprint that may be covered by a flammable vapor cloud as a result of an LNG release. Several new models have been used in recent years for this type of simulations. This prompted the development of the "*Model evaluation protocol for LNG vapor dispersion models*" (MEP): a procedure aimed at evaluating quantitatively the ability of a model to accurately predict the dispersion of an LNG vapor cloud.

This paper summarizes the MEP requirements and presents the results obtained from the application of the MEP to a computational fluid dynamics (CFD) model – FLACS. The entire set of 33 experiments included in the model validation database were simulated using FLACS. The simulation results are reported and compared with the experimental data. A set of statistical performance measures are calculated based on the FLACS simulation results and compared with the acceptability criteria established in the MEP. The results of the evaluation demonstrate that FLACS can be considered a suitable model to accurately simulate the dispersion of vapor from an LNG release.

1. Background

Liquefied natural gas (LNG) is a cryogenic liquid, obtained by cooling natural gas (primarily methane, with varying small percentages of ethane, propane and other gases) to approximately 111 K at atmospheric pressure. The liquefaction process reduces the specific volume of the natural gas by approximately 620 times, which allows large quantities of natural gas to be transported economically over long distances, primarily aboard large vessels (LNG carriers).

In the event of an accident – whether at an LNG liquefaction facility, on an LNG carrier or at a storage and regasification facility – hazardous conditions may occur that need to be carefully evaluated. The accurate prediction of the hazard area for an LNG release is challenging due to the complex physical phenomena that govern the evolution of such a scenario. Specifically, when the LNG spill reaches the ground (or the water) it forms a liquid pool that spreads by gravity but also boils vigorously due to the large temperature difference with the substrate. An accurate representation of the growth of the pool and of the rate of vapor formation (i.e., the "source term" to the vapor dispersion) are critical to estimate the hazard area for the flammable vapor cloud, particularly in situations where the pool growth may be affected by the terrain (e.g., spills into trenches).

Once the source term has been defined, the dispersion of the LNG vapor cloud needs to be calculated. An LNG vapor cloud is initially very cold (the boiling temperature of LNG is approximately 111.7 K) and dense (the density of methane vapors at boiling temperature is approximately 1.5 times the density of ambient temperature air). As a result, the vapor cloud tends to remain close to the ground and incurs limited mixing with ambient air, particularly at low-wind speeds (approximately less than 2 m/s). The vapor cloud dispersion can also be strongly affected by terrain features (e.g., slopes) and obstacles (e.g., storage tanks, buildings, dikes, etc.). An accurate representation of the LNG vapor cloud dispersion, therefore, requires a model that can account for all of these factors or, alternatively, can be demonstrated to be conservative in neglecting one or more of these factors.

Abbreviations: CFD, computational fluid dynamics; CHRC, Chemical Hazards Research Center; LFL, lower flammable limit; LNG, liquefied natural gas; LPG, liquefied petroleum gases; MEP, model evaluation protocol; MVD, model validation database; RANS, Reynolds-averaged Navier–Stokes; SPM, statistical performance measure.

* Corresponding author. Tel.: +1 301 915 9925.
E-mail address: fgavelli@gexcon.com (F. Gavelli).

0950-4230/$ – see front matter © 2010 Elsevier Ltd. All rights reserved.
doi:10.1016/j.jlp.2010.08.005

Nomenclature

Variables

f	friction coefficient [−]
h	thickness [m]
k	turbulent kinetic energy [m^2/s^2]
L	Monin–Obukhov length [m]
m	mass [kg]
q	Heat flux [W/m^2]
Re	Reynolds number [−]
T	temperature [K]
U	velocity [m/s]
u^*	friction velocity [m/s]
w^*	convective velocity scale [m/s]
z	elevation [m]
α	thermal diffusivity [m^2/s]
ε	turbulence dissipation rate [m^2/s^3]
λ	thermal conductivity [W/m K]
ν	kinematic viscosity [m^2/s]
ρ	density [kg/m^3]
θ	specific enthalpy [J/kg]
Ψ	stability function [−]

In recent years, several new models have been applied to perform hazard analyses for LNG vapor cloud dispersion scenarios, primarily to overcome some of the limitations of the earlier models (e.g., DEGADIS). In order to assess the capabilities of these models to accurately predict vapor cloud dispersion distances from LNG releases, a procedure was recently formalized in the "*Model evaluation protocol for LNG vapor dispersion models*" (Ivings, Jagger, Lea, & Webber, 2007).

The scope of this paper is to present the results obtained from the evaluation of a computational fluid dynamics (CFD) model – FLACS – according to the procedure outlined in the model evaluation protocol (MEP). In particular, the focus of this paper is on the validation of the FLACS model against the experimental data sets included in the MEP database. The paper will first introduce the MEP procedure and performance measures, then summarize the main features of FLACS. Next, the results of the FLACS validation effort will be presented and the model performance evaluated according to the MEP statistical performance parameters (SPM). Comments will also be provided, particularly to identify limitations of the MEP or areas for model improvement.

2. The model evaluation protocol (MEP)

The stated purpose of the MEP is to "provide a comprehensive methodology for determining the suitability of models to accurately simulate the dispersion of vapors emanating from accidental spills of LNG on land" (Ivings et al., 2007). The general approach followed in the MEP is based on earlier model validation work by Hanna (Hanna, Chang, & Strimaitis, 1993; Hanna, Strimaitis, & Chang, 1991) and by the Model Evaluation Group-Protocol (1994) and Model Evaluation Group-Guidelines (1994).

The specifics of the model evaluation protocol follow closely the structure of the SMEDIS project (Carissimo et al., 2001), revised and refined in order to be specific to the dispersion of LNG vapor clouds. Like the SMEDIS project, the MEP consists of three steps:

1. Scientific assessment. This step consists of a critical review of the physical, mathematical and numerical basis of the model being evaluated. The scientific assessment should be carried out by an independent third party, but interaction with the model developer is encouraged to ensure the details of the model are correctly understood. The MEP report includes a questionnaire that was developed to guide the scientific assessment process.
2. Model verification. This step consists of verifying the numerical implementation of the model from its mathematical description. The verification stage of the protocol is treated passively, as in the original SMEDIS protocol. This means that instead of carrying out a specific exercise to verify the model, evidence of model verification is sought from the model developer and then assessed by an independent third party, together with the scientific assessment.
3. Model validation. This step consists of comparing a model's prediction with experimental data. The goal of this step, as stated in the MEP report, is to determine whether a model can replicate "reality" to an acceptable degree.

In order for the validation step to be possible, a set of experimental data needs to be identified, that is both relevant to the purpose of the validation – that is, addresses the main physical phenomena affecting LNG vapor cloud dispersion – and whose test conditions (e.g., temperature, wind, spill characteristics) and measured data are defined with sufficient accuracy to allow meaningful model comparison. Following the criteria outlined in the MEP report, the "*Validation Database for Evaluating Vapor Dispersion Models for Safety Analysis of LNG Facilities*" (Coldrick, Lea, & Ivings, 2009) was assembled for this purpose. The model validation database (MVD) includes a total of 33 experimental data sets from large-scale field trials (15 sets) and wind-tunnel tests (18 sets), as summarized in Table 1. Four of the field trials series (Maplin Sands, Burro, Coyote and Falcon) consist of LNG spills onto water, while the other tests involved gaseous release of other dense gases (CO_2, SF_6, etc.). The majority of the field trials consisted of vapor cloud dispersion over mostly flat and unobstructed terrain, with the exception of the Falcon test series, in which the LNG spill occurred inside a fenced area. Therefore, the effect of obstructions was accounted for primarily in the wind-tunnel tests.

The model validation database (MVD) and associated guidance document contain summary information about the configuration of the 33 tests: ambient conditions (temperature, wind speed and direction) and release characteristics, as well as the experimental data against which model predictions should be compared. The experimental data included in the MVD, however, is limited to average ambient conditions over the duration of each tests and peak gas concentrations at specified locations; it does not include time traces at individual sensors (neither for ambient conditions nor for gas concentration), which could provide additional information when evaluating a model.

For the purpose of model evaluation, the database was separated into two groups: unobstructed and obstructed dispersion tests. While other grouping criteria could be applied and be helpful in evaluating a model, the choice made by the MEP authors was driven by the need to evaluate models with different capabilities: integral models (e.g., DEGADIS) that cannot account for the effect of obstructions can only be compared with tests from the unobstructed dispersion group (labeled "U" in Table 1), whereas CFD models would be capable of simulating both sets of tests.

The model evaluation protocol then defines a set of physical performance parameters, that is, physical quantities against which the performance of a model is to be evaluated. In the MEP, arc-wise data (i.e., data compared across several sensors distributed around an arc at a given distance from the source) are favored over point-wise data (i.e., data from individual sensors) because they are less affected by uncertainties in wind direction, that may cause lateral

Table 1
Experimental data sets in the model evaluation database.

Name	Sheet no.	Trial no.	Field or wind tunnel	Obstructed or unobstructed	Atmospheric stability class	Substance released
Maplin Sands 1980	1	27	F	U	C-D	LNG
	2	34			D	
	3	35			D	
Burro, 1980	4	3	F	U	B	LNG
	5	7			D	
	6	8			E	
	7	9			D	
Coyote, 1981	8	3	F	U	B-C	LNG
	9	5			C-D	
	10	6			D	
Falcon, 1987	11	1	F	O	G	LNG
	12	3			D	
	13	4			D-E	
Thorney Island 1982-84	14	45	F	U	E-F	Freon-12–nitrogen
	15	47			F	
CHRC, 2006	16	A	WT	U	D	Carbon dioxide
	17	B		O	D	
	18	C		O	D	
BA-Hamburg	19	Unobstructed (DA0120)	WT	U	D	Sulfur hexafluoride
	20	Unobstructed (DAT223)		U	D	
	21	Upwind fence (039051)		O	D	
	22	Upwind fence (039072)		O	D	
	23	Downwind fence (DA0501)		O	D	
	24	Downwind fence (DA0532)		O	D	
	25	Circular fence (039094/039095)		O	D	
	26	Circular fence (039097)		O	D	
	27	Slope (DAT647)		U	D	
	28	Slope (DAT631)		U	D	
	29	Slope (DAT632)		U	D	
	30	Slope (DAT637)		U	D	
BA-TNO	31	TUV01	WT	U	D	Sulfur hexafluoride
	32	TUV02		O	D	
	33	FLS		U	D	

meandering of the gas cloud. However, the fact that experimental data are collected at discrete crosswind locations makes cloud meandering an important factor in several field test simulations. The use of arc-wise physical comparison parameters in the MEP is consistent with both the SMEDIS project (Carissimo et al., 2001) and the model validation work by Hanna et al. (1993).

The most commonly used physical comparison parameter for arc-wise data in the literature is the maximum gas concentration across an arc, at a specific distance downwind from the release (Carissimo et al., 2001; Hanna et al., 1993; Hanna, Hansen, & Dharmavaram, 2004; Hansen, Melheim, & Storvik, 2007). This parameter allows evaluating how well a model predicts the downwind dispersion of a cloud, which ultimately affects the hazard distance prediction for a given accidental release. Therefore, most of the data sets in the MVD workbook include the arc-wise peak gas concentration experimentally measured at each available downwind arc. However, only the sensors located nearest the ground are included in the MVD data set, as it is argued that the highest concentration for a dense gas cloud will be at ground level. While the authors of this paper disagree with this blanket statement, especially in the case of vapor cloud dispersion over obstacles (e.g., vapor fences), the only possible comparison with reported data is by limiting the model's output to the same sensor locations included in the MVD.

As discussed by Hanna et al. (1993), the shortest averaging time available from the experimental data should be used to determine the maximum gas concentration, particularly when flammable vapor cloud dispersion is being considered. However, some models outputs are characteristic of long time averages and, as such, should be compared with similarly long time-averaged experimental results. Therefore, where possible, the MVD reports the experimental data for both short and long time averages, where short time averages are on the order of 1 s, whereas long time averages are comparable to the duration of the release. Additionally, a threshold of 0.1% gas concentration by volume was applied to the experimental data prior to inclusion in the MVD so that any recorded values below this threshold were omitted from the workbook.

Another parameter often discussed as a candidate to evaluate a model's performance is the downwind distance to the lower flammable limit (LFL), or to ½-LFL as U.S. federal regulations require for LNG facility siting purposes. However, the distance to LFL is not directly measured in the experiments but, rather, it is calculated by interpolation between measurements at successive arcs, which can be spaced over 100 m apart. Therefore, the reliability of the "experimental" distance to LFL was questioned by the authors of the MEP, who ultimately decided against including it as a physical comparison parameter.

Additional data is included in the MVD for several tests, such as the maximum cloud width or the cloud temperature at selected arc locations. This data can provide valuable additional information in the evaluation of a model's performance. However, the only physical comparison parameter consistently available throughout the model validation data set is the arc-wise peak gas concentration. Therefore, the FLACS model validation effort described in this paper will be focused on this parameter alone.

Quantitative model assessment criteria, based on the physical comparison parameters discussed earlier, are specified in the MEP in terms of a set of statistical performance measures (SPM) which compare model predictions with experimental measurements. The goal of the MEP SPMs is to provide a measure of bias (tendency to over/under predict the experimental results) and of spread (scatter around the average) in a model prediction. Once again, the MEP relies on previously published work (Carissimo et al., 2001; Hanna et al., 1993, 2004, 2007) to select the statistical performance measures as well as the associated quantitative assessment criteria. A summary of the SPM definitions and acceptability criteria is given in Table 2. For additional information, the reader is directed to the *Model evaluation protocol for LNG vapor dispersion models* (Ivings et al., 2007).

3. The FLACS CFD model

FLACS is a specialized CFD tool developed to address process safety applications such as:

- Dispersion of flammable or toxic gases;
- Gas and dust explosions;
- Propagation of blast and shock waves;
- Pool and jet fires.

For the purpose of simulating the dispersion of vapor clouds from liquefied natural gas (LNG) releases, FLACS provides an integrated environment where both the boiling, spreading liquid pool and the resulting vapor cloud dispersion are calculated simultaneously and while taking into account their respective interaction as well as the interaction with objects and terrain features. The following sections provide a brief description of the atmospheric dispersion and pool spreading and vaporization models.

3.1. The atmospheric dispersion model

FLACS calculates the atmospheric dispersion of gases and vapors by solving the three-dimensional (3D) Reynolds-averaged Navier–Stokes (RANS) equations on a non-uniform Cartesian grid, with the standard $k-\varepsilon$ model for turbulent closure (Launder & Spalding, 1974). Unlike most other commercial CFD models, FLACS uses the distributed porosity concept (Hjertager, 1986, chap. 41) to handle sub-grid objects (i.e., objects that are smaller than the grid cell size). This approach allows the simulation of dispersion in complex geometries, such as LNG liquefaction or regasification facilities, accurately and at much smaller computational costs than other CFD codes.

For atmospheric dispersion simulations, the atmospheric boundary layer is modeled by imposing profiles for velocity, temperature and turbulence on flow inlet boundaries. These profiles are specified as a function of the atmospheric stability (expressed according to the Pasquill–Gifford stability classes) and the surface roughness length, z_0. Logarithmic velocity profiles follow the derivation by van den Bosch (van den Bosch & Weterings, 1997) and can be written as:

$$U(z) = \frac{u^*}{\kappa}\left(\ln\left(\frac{z}{z_0}\right) - \psi_m\right) \tag{1}$$

where the friction velocity u^* is given by:

$$u^* = \frac{U_0\kappa}{\ln\left(\frac{z_{ref}}{z_0}\right) - \psi_m} \tag{2}$$

where U_0 is the velocity at the reference height z_{ref}. The stability function ψ_m is also given by van den Bosch (van den Bosch & Weterings, 1997) as:

$$\psi_m = \begin{cases} 2\ln\left(\frac{1+\xi}{2}\right) + \ln\left(\frac{1+\xi^2}{2}\right) - 2\arctan(\xi) + \frac{\pi}{2} & \text{for } L<0 \\ -17\left(1-\exp\left(-0.29\frac{z}{L}\right)\right) & \text{for } L>0 \end{cases} \tag{3}$$

where $\xi = (1-16z/L)^{1/4}$.

The temperature profile is assumed uniform. The expressions for the turbulent kinetic energy (k) and turbulence dissipation rate (ε) for neutral and stable atmospheric boundary layers follow the derivation by Han, Arya, Shen, and Lin (2000):

$$k(z) = \begin{cases} 6u^{*2} & \text{for } z \le 0.1h_{abl} \\ 6u^{*2}\left(1-\frac{z}{h_{abl}}\right)^{1.75} & \text{for } z > 0.1h_{abl} \end{cases}$$
$$\varepsilon(z) = \begin{cases} \frac{u^{*3}}{\kappa z}\left(1.24+4.3\frac{z}{L}\right) & \text{for } z \le 0.1h_{abl} \\ \frac{u^{*3}}{\kappa z}\left(1.24+4.3\frac{z}{L}\right)(1-0.85zh_{abl})^{1.5} & \text{for } z > 0.1h_{abl} \end{cases} \tag{4}$$

where h_{abl} is the height of the atmospheric boundary layer, which is typically on the order of 1000–1500 m for unstable boundary layers. For neutral or stable boundary layers, the boundary layer height is a function of the friction velocity u^*, the Coriolis parameter f_c, and the Monin–Obukhov length L as follows:

$$h_{abl,\text{neutral}} = 0.3\frac{u^*}{f_c}$$
$$h_{abl,\text{stable}} = 0.4\left(\frac{u^*L}{f_c}\right)^{1/2} \tag{5}$$

In unstable atmospheric boundary layers, heat flux from the ground induces vertical air flows that increase the turbulence level. These vertical flows can be parameterized by a convective velocity scale:

$$w^* = \left(\frac{g\dot{q}_g h_{abl}}{T_0\rho_\infty c_p}\right)^{1/3} \tag{6}$$

where $\dot{q}_g$ is the heat flux from the ground, T_0 and ρ_∞ denote reference temperature and density, respectively. The convective velocity scale is the most important parameter in determining the turbulence parameters in the atmospheric boundary layer, as discussed by Han et al. (2000):

$$k(z) = \begin{cases} 0.36w^{*2} + 0.85u^{*2}\left(1-3\frac{z}{L}\right)^{2/3} & \text{for } z \le 0.1h_{abl} \\ \left(0.36+0.9\left(\frac{z}{h_{abl}}\right)^{2/3}\left(1-0.8\frac{z}{h_{abl}}\right)^2\right)w^{*2} & \text{for } z > 0.1h_{abl} \end{cases}$$
$$\varepsilon(z) = \begin{cases} \frac{u^{*3}}{\kappa z}\left(1+0.5\left|\frac{z}{L}\right|^{2/3}\right)^{1.5} & \text{for } z \le 0.1h_{abl} \\ \frac{w^{*3}}{h_{abl}}\left(0.8-0.3\frac{z}{h_{abl}}\right) & \text{for } z > 0.1h_{abl} \end{cases} \tag{7}$$

Table 2
MEP statistical performance parameters and acceptability criteria.

Parameter	Definition	Acceptability criteria
Mean relative bias (MRB)	$\text{MRB} = \langle C_m - C_p / 0.5(C_m + C_p)\rangle$	$-0.4 < \text{MRB} < 0.4$
Mean relative square error (MRSE)	$\text{MRSE} = \langle (C_m - C_p)^2 / 0.25(C_m + C_p)^2\rangle$	$\text{MRSE} < 2.3$
Factor-of-2 fraction (FAC2)	$0.5 \le C_p/C_m \le 2.0$	$0.5 < \text{FAC2}$
Geometric mean bias (MG)	$\text{MG} = \exp\langle \ln(C_m/C_p)\rangle$	$0.67 < \text{MG} < 1.5$
Geometric variance (VG)	$\text{VG} = \exp\langle [\ln(C_m/C_p)]^2\rangle$	$\text{VG} < 3.3$

The atmospheric dispersion model in FLACS has been tested against a wide range of scenarios including releases of dense, passive and buoyant gases in open, obstructed and enclosed spaces (Dharmavaram, Hanna, & Hansen, 2005; Flaherty et al., 2007; Hanna et al., 2004; Hanna, Hansen, Ichard, & Strimaitis, 2009; Middha, Hansen, Grune, & Kotchourko, 2010).

3.2. LNG vapor source term – the pool spread and evaporation model

There are several possible ways to introduce gas or vapor in a FLACS dispersion simulation, depending on the physical characteristics of the release:

1. A gaseous release can be introduced in FLACS as a pure gas, or a gas/air mixture, at specified flow rate, velocity, turbulence and temperature. This approach is followed, for example, to simulate a jet from a gas leak in a pressurized system;
2. A superheated liquid release, for example from a leak in a pressurized liquid pipe, can be simulated in two different ways:
   a) By calculating the downwind distance after which the aerosol droplets have evaporated, and treating the release as a gas/air mixture from that location;
   b) By separating the flashing vapor and aerosol droplets at the actual source location and performing a two-phase dispersion calculation, accounting for heat and mass transfer between the phases;
3. A liquid release that would form a pool on the ground (or on water) can be simulated by calculating the spreading of the pool and the rate of vapor generation due to heat transfer from the surrounding environment (i.e., the pool substrate, solar radiation and ambient air).

In the model validation effort described in this paper, the gaseous release and the pool model source terms have been used, depending on the characteristics of the release.

In the case of liquid spills forming a pool, as in the case of low-pressure LNG releases, FLACS solves the two-dimensional (2D) shallow water equations to calculate the behavior of the pool. The assumption behind the shallow water theory is that the pool properties (temperature, velocity, etc.) are uniform across the thickness of the pool and, thus, are only a function of the horizontal coordinates (x, y). Therefore, the shallow water equations are an approximation of the equations of fluid motion, which is accurate when the thickness of the liquid pool is small in comparison with its horizontal dimensions. The advantage of using the 2D shallow water equations to calculate the pool spread and vaporization is that they account for the effect of terrain features (e.g., sloping, channels, etc.) or obstacles on the spread of the pool.

The shallow water equations for the conservation of mass and momentum are:

$$\frac{\partial h}{\partial t}+\frac{\partial h u_i}{\partial x_i}=\frac{\dot{m}_L-\dot{m}_V}{\rho_l}$$

$$\frac{\partial u_i}{\partial t}+u_i\frac{\partial u_i}{\partial x_j}=F_{g,i}+F_{\tau,i} \tag{8}$$

where $\dot{m}_L$ is the liquid spill rate into the pool and $\dot{m}_V$ is the rate of vaporization, and the terms on the right-hand side of the momentum equation represent the gravity and shear stress components, respectively:

$$F_{g,i}=g\Delta\frac{\partial(h+z)}{\partial x_i}$$

$$F_{\tau,i}=\frac{1}{8}f_t u_i|\vec{u}| \tag{9}$$

where $\Delta=1$ for pools spreading on solid surfaces and $\Delta=(1-\rho_l/\rho_w)$ for spills on water, and f_t is the friction coefficient between pool and substrate.

The rate of vaporization from the pool ($\dot{m}_V$) includes contributions from heat transfer from the substrate (e.g., ground or water), solar radiation and convective heat transfer from the air above the pool (Hansen et al., 2007). Fig. 1 shows a schematic of the heat transfer contributions modeled in the FLACS pool model.

The heat transfer components are factored into the energy equation, which is solved in terms of specific enthalpy, θ:

$$\frac{\partial\theta}{\partial t}+u_i\frac{\partial\theta}{\partial x_i}=\frac{\dot{m}_L}{h}(\theta_L-\theta)+\dot{q}_c+\dot{q}_{rad}+\dot{q}_g+\dot{q}_{evap} \tag{10}$$

where $\dot{q}_c$ is convective heat transfer, $\dot{q}_{rad}$ is heat transfer to the pool from radiation, $\dot{q}_g$ is heat transfer to the pool from the substrate, and $\dot{q}_{evap}$ is heat loss due to evaporation.

For cryogenic spills, heat transfer from the substrate is often the main source of heat input to the pool. In the FLACS pool model, heat transfer from a solid substrate (e.g., ground) is calculated as a function of position and time according to the semi-infinite solid heat transfer theory, assuming perfect contact between pool and substrate (Incopera & de Witt, 1996, chap. 5):

$$q_s(x,y,t)=\frac{\lambda_s\left(T_s^0-T_l\right)}{\sqrt{\pi\alpha_s(t-t_w(x,y))}} \tag{11}$$

where λ_s and α_s are the thermal conductivity and thermal diffusivity of the substrate, T_s^0 is the initial temperature of the substrate, T_l is the temperature of the pool and t_w is the time at which the substrate (at position x, y) is first wetted by the LNG. Heat transfer to an LNG pool spreading on water is more difficult to calculate, due to the complex phenomena associated with pool boiling, combined with the convective motion of the water beneath the pool, the turbulent behavior of the LNG/water interface and the possibility of waves or currents. Experimental data from laboratory and field tests have shown that heat transfer increases significantly when the LNG pool is spreading, primarily due to turbulence at the interface between LNG and water. In order to capture the effect of pool motion and turbulent mixing on the local heat transfer, an approach similar to Rohsenow's superposition model (Rohsenow, 1952) is followed, where the total heat transfer to the pool is the sum of a pool boiling term and a forced convection term. The total heat transfer to the pool, therefore, is a function of the relative motion of the pool with respect to the water substrate, which is expressed in terms of the local Reynolds number:

$$Re_h=U\,h/\nu \tag{12}$$

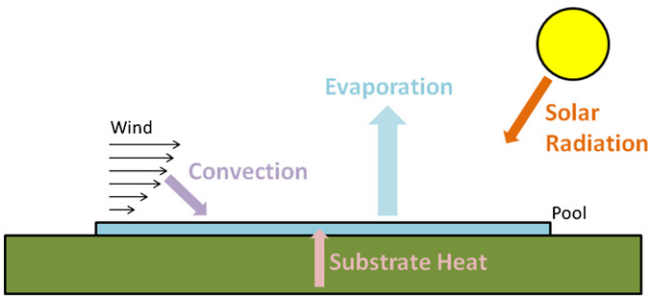

Fig. 1. Schematic of the pool heat transfer in FLACS.

where U is the local relative velocity, h is the local thickness of the pool and ν is the kinematic viscosity of LNG.

The 2D shallow water equations are solved at every time step and on the same computational domain as the atmospheric flow. This allows the heat transfer from the ambient to be accounted for in a realistic and time-dependent manner.

3.3. The FLACS modeling approach

The atmospheric dispersion of a dense cloud is affected by terrain features and obstacles. Therefore, it is important for a model to be able to reproduce the features within the computational domain as accurately as possible in order to minimize modeling errors due to geometry approximations. In the FLACS simulations included in this paper, the geometry was defined according to the information provided in the model validation database (MVD) guide, supplemented in some cases by information from test-specific literature (e.g., test reports). Therefore, the main geometry features for each test were included in the FLACS simulations, however, smaller details – such as small terrain undulations – may not have been fully represented due to insufficient information being provided.

Atmospheric boundary layer profiles for wind velocity, turbulent kinetic energy and turbulent dissipation rate were set at the inflow and side boundaries, according to the Pasquill–Gifford stability class specified in the MVD for each field test; deviations from this procedure will be discussed in the test-specific sections below. In the simulations of the wind-tunnel tests, instead, the inflow conditions were defined using a logarithmic wind profile with 5–10% turbulence intensity and a turbulent length scale 1–2 times the smallest grid cell size dimension as typical for CFD simulations of these scenarios. A passive outflow condition at ambient pressure was set at the exit boundaries for all tests. Other boundary conditions, such as average wind direction, ambient temperature and surface roughness length, were specified according to the information in the MVD for most tests; deviations from this practice will be discussed in the test-specific sections below.

One of the goals in the development of FLACS is to minimize user dependency of the simulation results. Since FLACS includes a single turbulence closure model and grid scheme, the only area of a simulation where user dependency may affect the results – assuming that the geometry and test conditions are well specified – is in the specification of the grid cell size, particularly in proximity of the vapor source. For this reason, in addition to the "standard" CFD meshing guidelines, such as ensuring that the domain boundaries do not affect the flow in the region of interest or that cells with large aspect ratios are avoided in areas where strong gradients are expected, FLACS users are provided with a set of validation-based guidelines for mesh generation. Among these guidelines, which may be found in the FLACS User's Manual (FLACS v9.1 User's Manual, 2009), the following are most relevant to the specific simulations included in this paper:

- Release sources must be properly resolved: FLACS meshing guidelines recommend a minimum of 10 grid cells across the initial diameter of a liquid pool, whereas high-pressure gas releases must be resolved with grid cells slightly larger than the area of the expanded jet.
- Horizontal grid aspect ratios should not be greater than 1:5 near the vapor source and in region of high velocity gradients. Larger grid aspect ratios (up to a maximum of approximately 1:100) can be used further away from the source and where flow gradients are smaller. Grid stretching factors should be kept to 1.2 or less, except for local refinement near high-pressure jets where a stretching factor of 1.4 is acceptable.
- Grid cells smaller than 1 cm should be avoided. If grid cells smaller than 1 cm are used, a sensitivity study should be performed to ensure results are not affected by the small grids.
- When simulating dense gas dispersion, the vertical grid size near the ground should be less than the height of the lowest sensors (i.e., the sensors should not be within the first layer of grid cells near the ground).

Another important modeling consideration, particularly for field trial simulations, is whether the reported average boundary conditions, particularly wind speed and direction, are representative of the actual conditions during the test, or whether they should be replaced by time-dependent data at individual measuring stations. For example, Fig. 2 compares the actual wind speed and direction during the Burro 8 test (as recorded by a sensor placed 150 m upwind of the LNG spill and 2 m above ground) with their respective averages as reported in the MVD. It is evident, in this case, how the average values do not provide an accurate representation of the actual test conditions. In fact, more than a factor of two difference in the peak gas concentration at the first arc of sensors was obtained when simulating the same test with the two sets of boundary conditions (see Fig. 3).

The difference in the results may often be caused by wind "meandering": a steady wind could direct the cloud through the gap between two sensors (which are spaced tens of meters apart in the crosswind direction), whereas side-to-side fluctuations would tend to spread the cloud crosswind allowing it to "hit" more sensors (Hanna et al., 2004). Wind speed fluctuations are also likely to have a strong effect on the downwind dispersion of the cloud, especially in stable and low-wind atmospheric conditions. For example, it is generally observed that for wind speeds below approximately 2 m/s (measured at 2 m above ground), a dense cloud tends to remain low

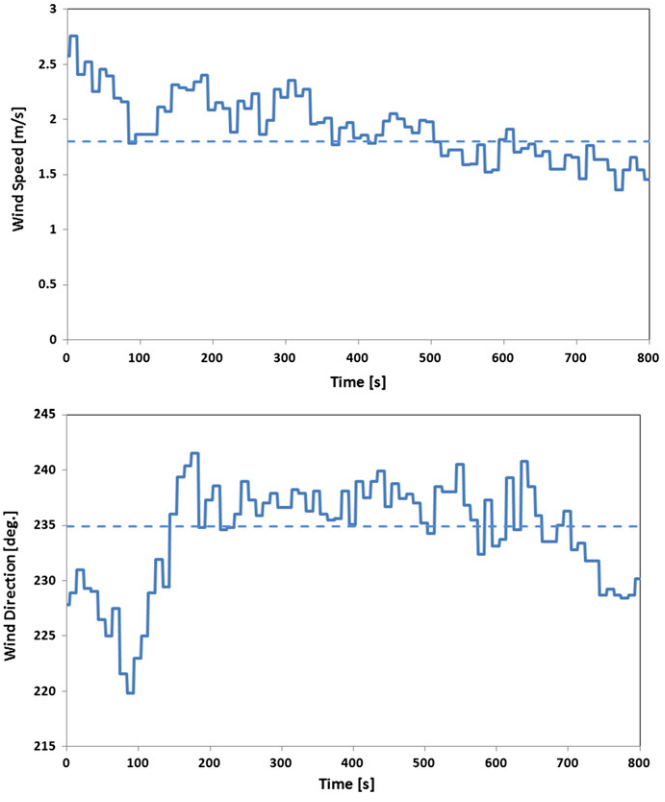

Fig. 2. Experimentally measured wind speed (top) and direction (bottom) for Burro 8: time traces (solid lines) versus reported averages (dashed lines).

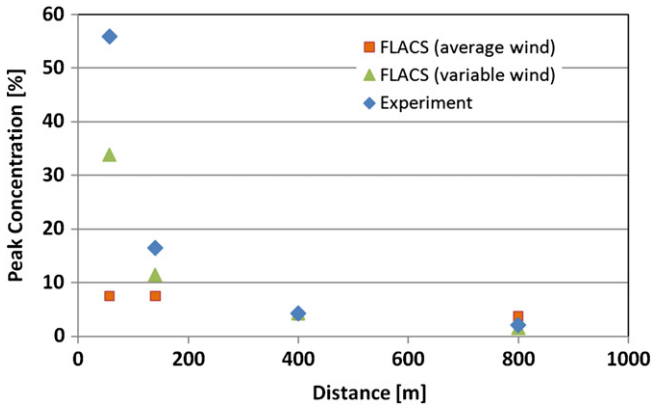

Fig. 3. Comparison of FLACS predictions for Burro 8 using the MVD-reported average wind conditions (orange squares) or the actual sensor data (green triangles). Experimental data are also included for reference (blue diamonds). (For interpretation of the references to color in this figure legend, the reader is referred to the web version of this article.)

to the ground and is advected by the wind while mixing very slowly; on the other hand, winds above 2 m/s tend to make the cloud "taller" and significantly increase mixing. Therefore, when simulating a test like Burro 8, which has average wind speed of less than 2 m/s but actual wind speed exceeding 2 m/s for part of the cloud dispersion phase, the "simpler" average boundary conditions can lead to significant prediction errors.

4. FLACS validation against the MEP database

As discussed earlier, information on the tests included in the MEP validation database is provided in the *Guide to the LNG Model Validation Database* (Coldrick et al., 2009). The information is summarized in a Microsoft Excel workbook which includes, for each test in the database, ambient and spill conditions, peak gas concentration measurements at several locations and, in some cases, temperature measurements. For the wind-tunnel tests, gas concentration measurements are provided both at wind-tunnel scale and at full scale, so the modeler can choose whether to simulate the actual wind-tunnel test or the scaled-up scenario. For each test, the model predictions can be entered so that the statistical performance parameters are calculated automatically.

The following sections present the FLACS simulation results for all 33 tests in the MEP database. The comparison with experimental data is performed according to the procedure outlined in the MEP report – that is, by comparing peak gas concentration at specified arcs and calculating the statistical performance measures (SPM). As discussed earlier, additional analysis of the model predictions could be performed – for example, by comparing with experimental traces at individual sensors – but such effort is beyond the requirements of the MEP as well as the scope of this paper.

Even though FLACS is a RANS-based code, it uses a low Mach number compressible solver which is characterized by small time steps, resulting in short time averages for the results. Therefore, FLACS model predictions will be compared against short time average experimental results (where these are available in the MVD).

In order to keep consistency with the organization of the MEP, the FLACS simulation results are separated into two groups, as follows:

- Group 1: Unobstructed dispersion.
  - ○Field test series: Maplin Sands; Burro; Coyote; Thorney Island.
  - ○Wind-tunnel test series: CHRC Case A; BA-Hamburg (unobstructed and sloped); BA-TNO (unobstructed).
- Group 2: Obstructed dispersion.
  - ○Field test series: Falcon.
  - ○Wind-tunnel test series: CHRC Cases B-C; BA-Hamburg (with fence); BA-TNO (with fence).

4.1. Group 1: unobstructed dispersion data sets

4.1.1. Maplin Sands test series

The Maplin Sands trials were conducted by Shell Research Limited in 1980 and consisted of 34 spills of liquefied gases onto the sea (Colenbrander, Evans, & Puttock, 1984a, 1984b, 1984c). Both continuous and instantaneous releases of LNG and LPG were carried out through a vertical pipe terminating above the water surface. No "splash plate" was used to divert the flow and prevent it from penetrating the water surface. The site was located in an area of tidal sands in the Thames estuary, so the cloud dispersion occurred over flat terrain. Instruments were arranged in several arcs around the spill location, between approximately 90 and 650 m radius.

The MEP identified a subset of three tests from the Maplin Sands series as suitable for model validation purposes. All three tests consist of continuous LNG releases, under medium-to-high wind speeds, as summarized in Table 3.

The FLACS model for the Maplin Sands tests was setup according to the information included in the MEP, supplemented by information from other sources (Colenbrander et al., 1984c; Ermak, Chapman, Goldwire, Gouveia, & Rodean, 1988; Hanna et al., 1993; Puttock, Blackmore, & Colenbrander, 1982). The LNG vapor source term was calculated using the FLACS pool model. The computational domain for vapor dispersion stretched from −300 to 900 m in the direction of the wind, from −250 to 250 m in the crosswind direction and from sea level to 100 m elevation. The grid resolution in the near field was 1 m × 1 m × 0.33 m and was stretched progressively away from the spill. The total grid cell count was approximately 315,000.

An example of the FLACS simulation is provided in Fig. 4, which shows the LNG vapor cloud (color-coded according to gas concentration by volume) at 0.8 m elevation for test MS 27. The long and narrow cloud shape is characteristic of dispersion under steady and medium-to-high winds. For the same test, Fig. 5 compares the predicted and measured peak gas concentration at several distances from the spill. The results show an excellent correlation between simulation and experimental results for this test. Similar results were obtained for the other Maplin Sands tests included in the MEP database, as the correlation plot in Fig. 6 demonstrates: 100% of simulation results fall well within the "factor-of-2" range (the region between the dashed lines in the figure) with respect to the experimental data.

4.1.2. Burro tests series

The Burro series of experiments were performed at the Naval Weapons Center, China Lake, California in 1980 (Koopman, Baker, et al., 1982; Koopman, Cederwall, et al., 1982; Goldwire et al., 1983). LNG was spilled onto the surface of a 58 m diameter water

Table 3
Maplin Sands tests included in the MEP database.

Test no.	Wind speed (m/s)	Material	Spill flow (kg/s)	Spill duration (s)
MS 27	5.5	LNG	23.2	160
MS 34	8.6	LNG	21.5	95
MS 35	9.8	LNG	27.1	135

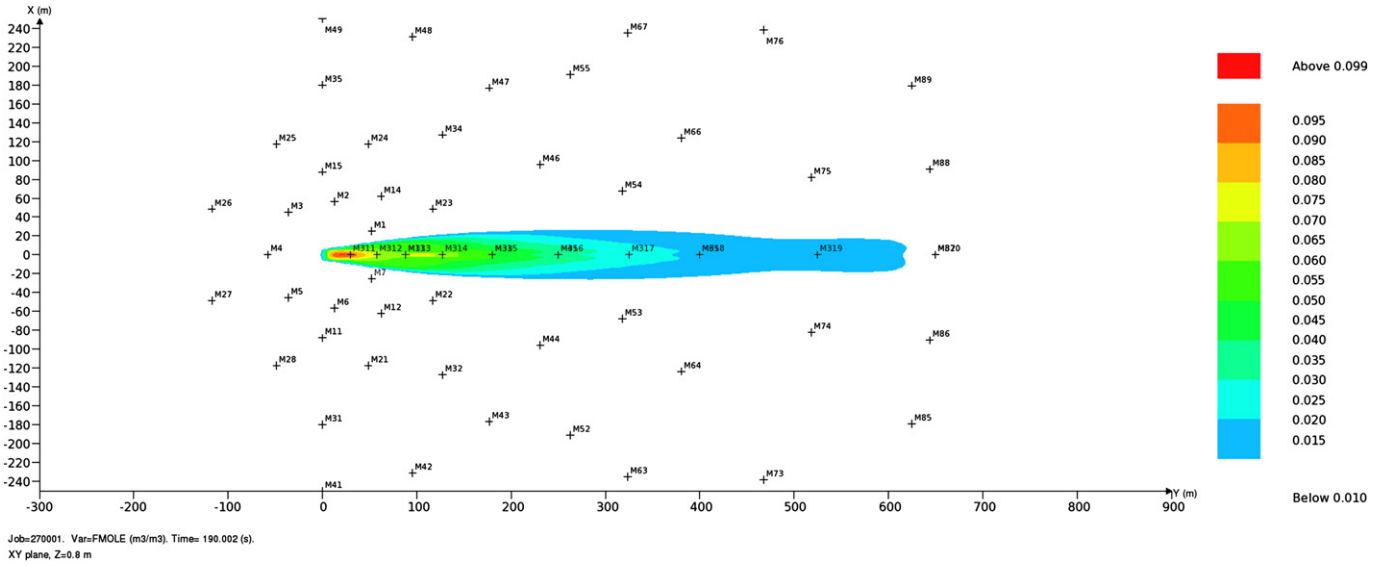

Fig. 4. Steady-state plume for test MS 27.

pond, whose surface was approximately 1.5 m below ground level. A splash plate was located just below the water surface to redirect the flow of LNG horizontally. The terrain downwind of the spill pond sloped upward at about 7° for 80 m, before leveling out to about a 1-degree slope. Gas concentration measurements were performed along arcs at 57, 140, 400 and 800 m downwind from the spill. The array centerline was aligned with the prevailing wind direction.

The MEP identified a subset of four tests from the Burro series as suitable for model validation purposes. The test conditions are summarized in Table 4.

The LNG pool spread and vaporization were simulated using the FLACS pool model. The terrain features of the China Lake test site were neglected and the terrain downwind of the spill pond was assumed to be flat. While terrain features could affect the dense cloud dispersion, particularly for the lowest wind speed tests (e.g., Burro 8), the flat terrain assumption is frequently made when simulating the Burro tests. The most severe impact on the Burro series modeling results, instead, was found to be associated with the boundary conditions specified in the MVD. As discussed earlier, the MVD reports only the average wind speed and direction for each test; however, in some cases the average values may not be representative of the actual test conditions – for example, if the wind direction fluctuates or the wind speed decreases throughout the test, as in the case of Burro 8 (see Fig. 2). Based on the Burro 8 simulation results and the observation of the wind speed and direction data for the other Burro tests, it was decided that wind meandering was likely an important factor to consider in all four Burro tests included in the MVD. Therefore, variable wind was implemented in all four cases.

Another deviation from the test boundary conditions specified in the MVD was made for the Burro 3 test: the atmospheric stability class specified in the MVD (Pasquill–Gifford class B, or "unstable") was replaced with a neutral profile (class D), to avoid some limitations in the handling of unstable atmospheric profiles in the current version of FLACS. Since atmospheric stability tends to decrease mixing, performing a simulation with a more stable atmospheric boundary layer profile tends to produce conservative results – that is, longer downwind dispersion distances.

The computational domain for vapor dispersion stretched from −100 to 1000 m in the direction of the wind, from −200 to 200 m in

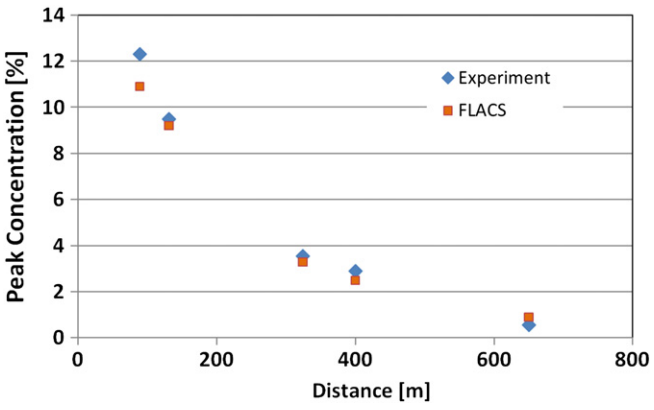

Fig. 5. Measured versus predicted concentrations for test MS 27.

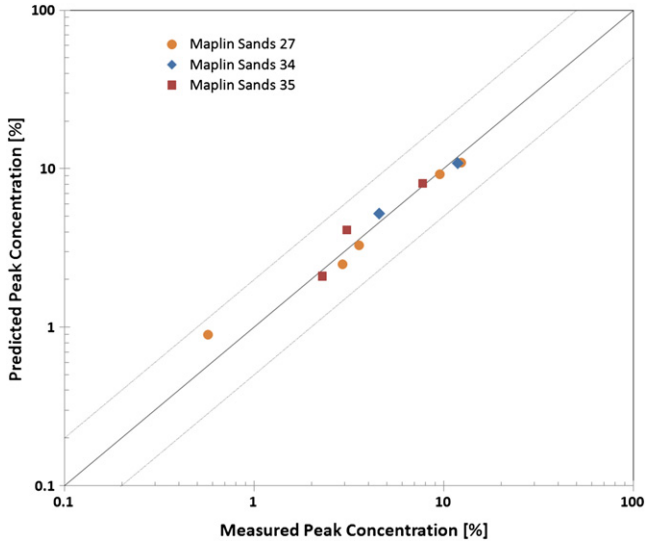

Fig. 6. Comparison of predicted to measured gas concentration for the Maplin Sands tests.

Table 4
Burro tests included in the MEP database.

Test no.	Wind speed (m/s)	Material	Spill flow (kg/s)	Duration (s)
3	5.6	LNG	88	167
7	8.8	LNG	99	174
8	1.8	LNG	117	107
9	5.9	LNG	136	79

the crosswind direction (except the Burro 8 simulation, where the domain spanned −400 to + 200 m due to the wind direction) and from the water pond level (−1.5 m) to 50 m elevation. The grid resolution in the near field was 1 m × 1 m × 0.5 m and was stretched progressively away from the spill. The total grid cell count was approximately 430,000.

An example of the FLACS simulation is provided in Fig. 7, which shows a snapshot of the LNG vapor cloud (color-coded according to gas concentration by volume) at 0.8 m elevation for test Burro 8. The vapor cloud is much more "round" than in the Maplin Sands test shown previously (Fig. 4), as expected when a dense cloud is dispersed under low-wind speeds. The upwind slumping of the LNG cloud is also noticeable and consistent with the observations by Koopman, Baker, et al. (1982). The predicted distance to the lower flammable limit (LFL) for the Burro 8 test is approximately 400 m, within approximately 5% of the value calculated from the experimental data (420 m). The correlation plot in Fig. 8 shows that 92% of simulation results from the four Burro tests fall within the "factor-of-2" range with respect to the experimental data.

4.1.3. Coyote test series

The Coyote test series was a follow-up to the Burro tests and was aimed at studying LNG vapor cloud fires, as well as the Rapid Phase Transition (RPT) phenomena that had been observed in the Burro tests (Goldwire et al., 1983). The Coyote tests were performed on the same test facility (China Lake) as the Burro tests but, given their different scope, most sensors were relocated to the 140 m and 400 m arcs to gather data closer to the spill location.

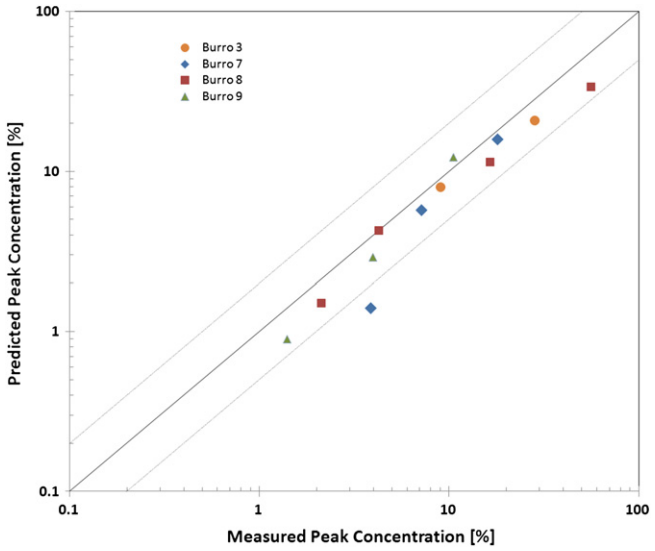

Fig. 8. Correlation of simulated to experimental gas concentration for the Burro tests.

The MEP identified a subset of three tests from the Coyote series as suitable for model validation purposes. The test conditions are summarized in Table 5.

Similar to the Burro test series, the LNG vapor source term from the spreading LNG pool was calculated using the FLACS pool model and the terrain was modeled as a flat surface. Wind meandering was imposed at the flow inlet boundaries, as in the Burro tests. Tests 3 and 5 were reported in the MVD to have unstable or slightly unstable atmospheres (Pasquill–Gifford classes B or C, respectively); these tests were simulated with a neutral atmosphere (class D) in accordance with current FLACS user recommendations, to avoid the unstable atmosphere handling issues described previously.

Also similar to the Burro simulations, the computational domain for vapor dispersion stretched from −100 to 600 m in the direction of the wind, from −200 to 200 m in the crosswind direction and

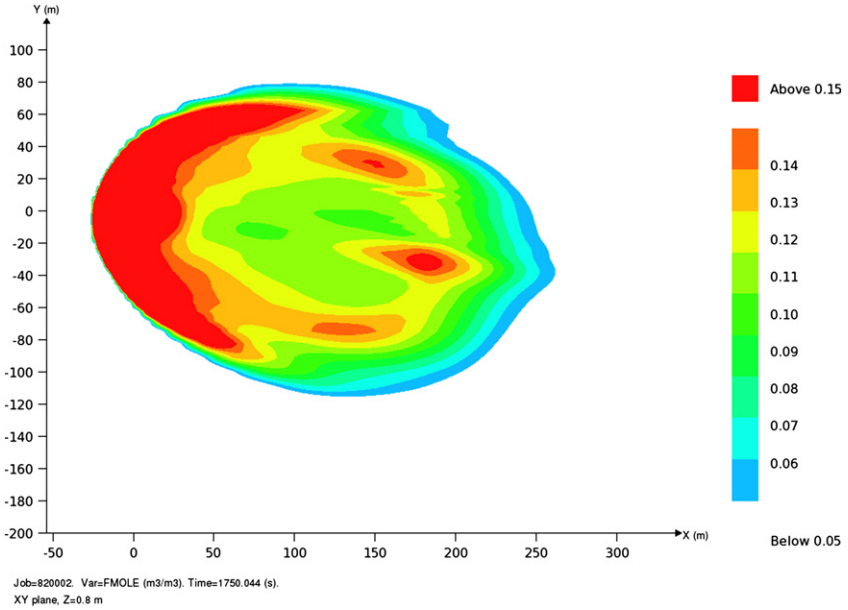

Fig. 7. Snapshot of the LNG vapor cloud for test Burro 8.

Table 5
Coyote tests included in the MEP database.

Test no.	Wind speed (m/s)	Material	Spill flow (kg/s)	Duration (s)
3	6.8	LNG	101	65
5	10.5	LNG	129	98
6	5.0	LNG	123	82

from pond level (−1.5 m) to 50 m elevation. The grid resolution in the near field was 1 m × 1 m × 0.5 m and was stretched progressively away from the spill. The total grid cell count was approximately 335,000.

An example of the FLACS simulation is provided in Fig. 9, which shows the LNG vapor cloud (color-coded according to gas concentration by volume) at 1 m elevation for test Coyote 5. For the same test, Fig. 10 compares the predicted and measured peak gas concentration at several distances from the spill. The results show an excellent correlation between simulation and experimental results for this test. Similar results were obtained for the other Coyote tests included in the MEP database, as the correlation plot in Fig. 11 demonstrates: 91% of simulation results fall within the "factor-of-2" range with respect to the experimental data.

4.1.4. Thorney Island test series

The Heavy Gas Dispersion trials at Thorney Island were performed by the British Health and Safety Executive to study the dispersion of heavy gas releases, using a mixture of freon-12 and nitrogen (McQuaid, 1987). The tests were performed at a former Royal Air Force station, therefore, the test area was largely clear and mostly flat. Both instantaneous and continuous releases were performed. For the continuous release tests, the gas mixture was delivered through a vertical duct emerging at ground-level beneath a 2 m diameter cap, located 0.5 m above the ground. This

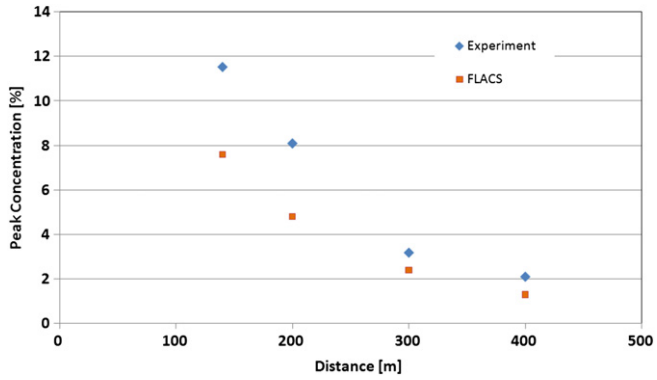

Fig. 10. Measured versus predicted concentrations for test Coyote 5.

arrangement was designed to release the gas with near-zero vertical momentum. The instrumentation was mounted on 38 fixed towers, each with five gas sensors. The far-field sensors (over 250 m away from the release) were on a uniform grid, spaced 100 m; a more concentrated array of sensors was used in the near field. The model validation database (Coldrick et al., 2009) does not specify the elevation of the sensors, but other sources indicate that the lower sensors were placed 0.4 m above ground (Hanna et al., 1993). The MEP identified two tests from the Thorney Island series as suitable for model validation purposes. The test conditions are summarized in Table 6.

The computational domain for vapor dispersion stretched from −300 to 100 m in the *x*-direction, from −50 to 500 m in the *y*-direction and from ground level to 25 m elevation. The grid resolution in the near field was 0.8 m × 0.8 m × 0.25 m and stretched progressively away from the release. The total grid cell count was approximately 285,000.

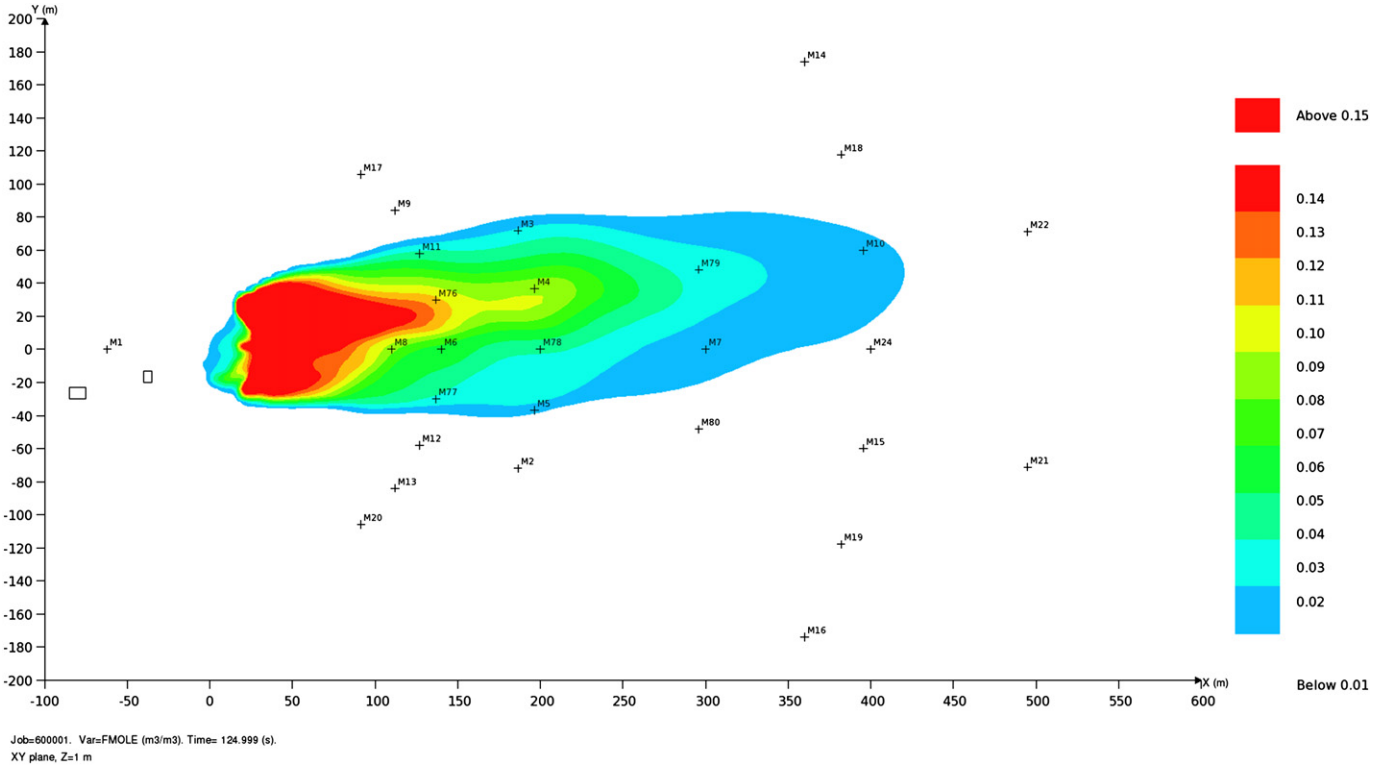

Fig. 9. Steady-state plume for test Coyote 5.

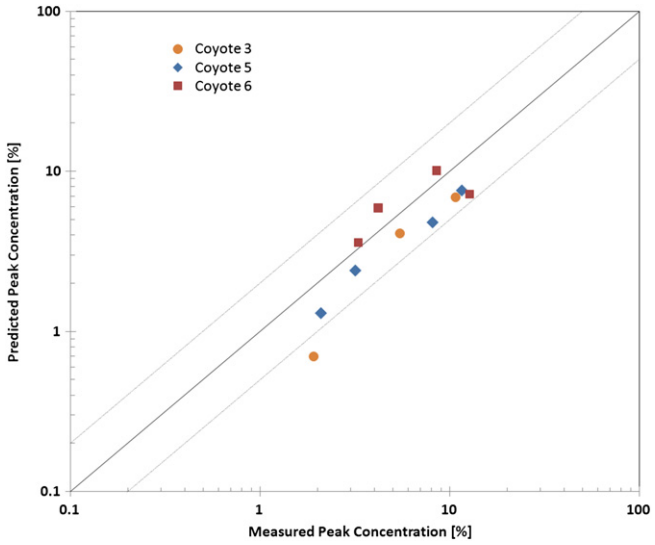

Fig. 11. Correlation of simulated to experimental gas concentration for the Coyote tests in the MEP database.

The elevation of the sensors was not specified in the MVD, therefore, the FLACS simulations were performed with two identical arrays of sensors – one near the ground (0.1 m) and one at 0.4 m elevation. The near field data correlated very closely with the ground-level sensors, as shown in Fig. 12. Given the proximity of the sensors to the ground, it is likely that the presence of brush or other minor terrain non-uniformities may affect the wind profile near the ground in a more complex manner than can be replicated using a simple surface roughness parameter. Also, as shown in Table 6, these tests were performed under low-wind speed conditions but, unlike the Burro tests, no sensor data was available to determine whether wind fluctuations may have occurred that could have affected the cloud dispersion. As in the Burro tests, the pancake cloud shape and upwind dispersion are consistent with dense gas dispersion under low-wind speeds. Also interesting is the "plow" or "half-moon" shape of the gas cloud in the near field, which causes the highest gas concentration to be near the edges of the plow instead of along its centerline. This phenomenon can explain the following observation made by Ermak et al. (1988): "The pattern of gas concentration data suggests that the cloud moved along the axis of the instrument array (0°) for about 30–50 m before it turned to the left and moved along the general direction of the wind direction (−32.6°)." In fact, what Ermak et al. may have observed is the higher gas concentration near the edges of the cloud reaching one of the sensors along the 0-degree direction, as Fig. 12 indicates.

Fig. 13 compares the predicted and measured peak gas concentration at several distances from the release, also for test TI47. The results show an excellent correlation between simulation and experimental results for this test, with the caveat that the sensor elevation was changed to 0.1 m, as discussed above. Similar results were obtained for the other Thorney Island test included in the MEP database (TI45), as the correlation plot in Fig. 14 demonstrates: 85% of simulation results fall within the "factor-of-2" range with respect to the experimental data.

Table 6
Thorney Island tests included in the MEP database.

Test no.	Wind speed (m/s)	Material	Spill flow (kg/s)	Duration (s)
45	2.3	Freon-12 –nitrogen	10.7	455
47	1.5	Freon-12 –nitrogen	10.2	465

4.1.5. CHRC test A

The Chemical Hazards Research Center (CHRC) at the University of Arkansas performed a series of wind-tunnel experiments on the dispersion of CO_2 over rough surfaces, with and without obstacles (Havens & Spicer, 2005, 2006; Havens, Spicer, & Sheppard, 2007). The CHRC facility is an ultra low-speed boundary layer wind tunnel with a 2.1 m by 6.1 m by 24.4 m long test section. The wind-tunnel floor consisted of rubber matting with mounted roughness elements, to give turbulence properties consistent with field-scale scenarios. The CHRC wind-tunnel experiments were at a scale of 1:150 and consisted of the three cases summarized in Table 7.

Test A is the only unobstructed dispersion test performed by CHRC. Tests B and C will be discussed in the obstructed dispersion tests section (Group 2). Room-temperature CO_2 was released continuously, at a rate of 33.4 L/min with 0.5 L/min of propane added as a tracer, through a square-shaped area with a central circular section blanked-off. The wind speed was 0.4 m/s at a reference height of 6.7 cm. Gas concentration measurements were made at an elevation of 0.5 cm, at several downwind distances from the source and with 10 cm crosswind spacing.

The FLACS simulations were performed at wind-tunnel scale. The gas was injected into a cavity below ground, covered by a plate with 50% vertical porosity. The terrain downwind of the release was assumed to be flat and 3 cm by 3 cm plates were added to replicate the roughness elements in the wind tunnel. A logarithmic wind profile was specified at the wind-tunnel inlet, with 5% turbulence intensity and 3 mm turbulence length scale (equal to the smallest grid cell size).

The computational domain for vapor dispersion stretched from −1 to 6 m in the wind direction, from −1.5 to 1.5 m in the crosswind direction and from ground level to 1 m elevation. The grid resolution in the near field was 30 mm by 30 mm by 3 mm and stretched progressively away from the release. The total grid cell count was approximately 245,000. In order to properly resolve the vertical gradients and the sensor spacing, the grid selection did not meet the FLACS meshing guidelines, which recommend a minimum grid cell size of 10 mm and a maximum aspect ratio of 5 in proximity of the release. However, a sensitivity run performed using a guideline-compliant mesh provided comparable results and verified the adequacy of the smaller mesh. An alternative approach could have been followed by performing the simulation at the 150:1 "field" scale.

An example of the FLACS simulation is provided in Fig. 15, which shows the steady-state CO_2 cloud (color-coded according to gas concentration by volume) at 5 mm elevation. The three-pronged contours in the figure are likely an artifact of the source definition (array of 3×3 point releases). A finer mesh of release sources in the horizontal directions may result in smoother downwind contours. The correlation plot in Fig. 16 shows that 100% of simulation results fall within the "factor-of-2" range with respect to the experimental data.

4.1.6. BA-Hamburg unobstructed tests

The BA-Hamburg trials were conducted in an open circuit wind tunnel at the Meteorological Institute of the University of Hamburg (Nielsen & Ott, 1996). The wind-tunnel test section measures 1.5 m by 1 m and is 4 m long. Irwin spires and distributed roughness elements (2 cm high Lego blocks) are installed in the flow establishment section to generate a turbulent boundary layer profile. The trials included in the model validation database consisted of long duration floor-level releases of sulfur hexafluoride (SF_6) gas at room

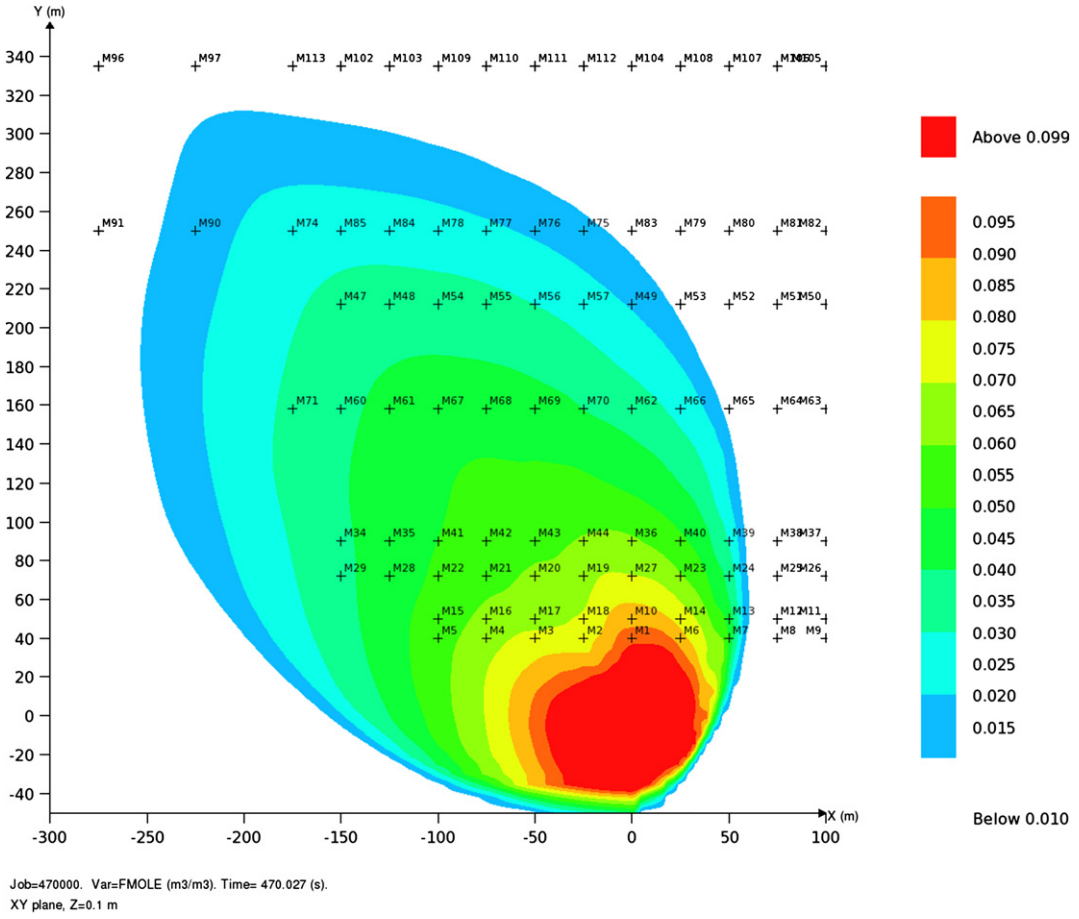

Fig. 12. Steady-state plume for test TI47 ($z = 0.1$ m).

temperature. The gas was introduced through a perforated disk, approximately 7 cm in diameter and mounted flush with the tunnel floor. The experiments were at a scale of 1:164. Gas concentration measurements were made at floor level using an aspirated film probe.

Several tests were performed in the BA-Hamburg series, using different configurations. In this section, the results for the unobstructed dispersion tests are discussed; the obstructed tests will be discussed with the Group 2 data sets.

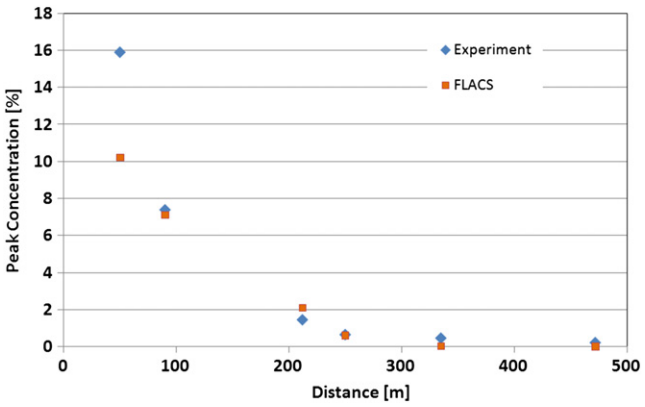

Fig. 13. Measured versus predicted concentrations for test TI47.

4.1.6.1. Flat terrain, horizontal. The MVD includes two tests from the BA-Hamburg series (DAT0120 and DAT223), in which gas dispersion occurred over flat, horizontal and unobstructed ground. Given the small dimensions of the wind tunnel, the FLACS simulations of these tests were performed at "field" scale in order to

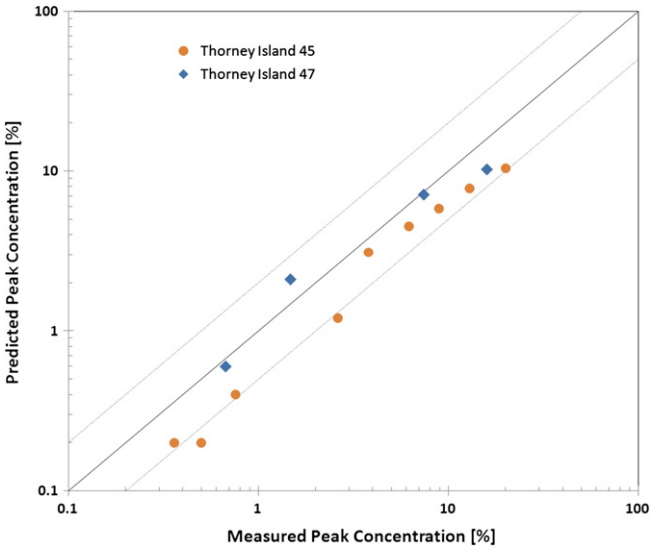

Fig. 14. Correlation of simulated to experimental gas concentration for the Thorney Island tests.

Table 7
CHRC wind-tunnel tests included in the MEP database.

Test no.	Features	Wind speed (m/s)	Material	Release flow (l/min)	Duration (s)
A	Unobstructed	0.4	CO_2	33.4	Continuous
B	Tank and Dike	0.4	CO_2	33.4	Continuous
C	Dike only	0.4	CO_2	33.4	Continuous

comply with the FLACS meshing guidelines. The gas source was specified as a diffusive leak from a cylindrical hole of 11.2 m diameter, covered by a plate with 50% vertical porosity. The ground was assumed to be flat and sensors were defined at ground level (5 cm elevation in field scale) along the axis of the tunnel. A logarithmic wind was specified at the inlet boundary, with 5% turbulence intensity and turbulence length scale equal to the smallest grid cell size.

The computational domain for vapor dispersion stretched from −80 to 480 m in the wind direction, from −75 to 75 m in the crosswind direction and from −3 to 25 m elevation (the negative elevation was necessary to accommodate the gas leak volume). The grid resolution in the near field was 1 m by 1 m by 0.2 m and stretched progressively away from the release. The total grid cell count was approximately 240,000.

An example of the FLACS simulation is provided in Fig. 17, which shows the gas cloud (color-coded according to gas concentration by volume) at 0.1 m elevation for test DAT0120. For the same test, Fig. 18 compares the predicted and measured peak gas concentration at several distances from the spill. The results show an excellent correlation between simulation and experimental results for this test.

4.1.6.2. Unobstructed, sloped ground tests. The MVD also includes a set of four tests from the BA-Hamburg series (DAT647, 631, 632 and 637), in which the unobstructed tunnel floor was sloped downwards away from the release location. These tests were also simulated at field scale and with a similar setup (mesh size, etc.) to the flat terrain tests. In order to account for the sloping terrain, the direction of the gravity was adjusted accordingly.

An example of the FLACS simulation is provided in Fig. 19, which shows the gas cloud (color-coded according to gas concentration by volume) at 0.1 m elevation for test DAT637. For the same test, Fig. 20 compares the predicted and measured peak gas concentration at several distances from the spill. The results show an excellent correlation between simulation and experimental results for this test.

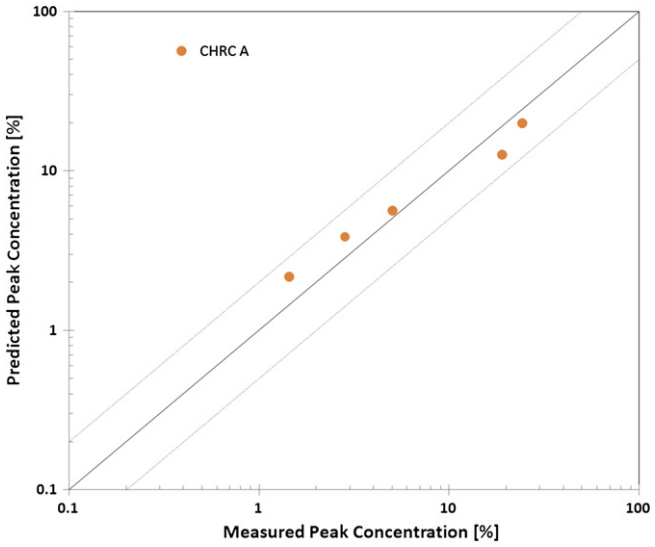

Fig. 16. Correlation of simulated to experimental gas concentration for test CHRC − A.

A summary of the results from the simulation of the six unobstructed BA-Hamburg tests is given by the correlation plot in Fig. 21. The plot shows that 79% of simulation results fall within the "factor-of-2" range with respect to the experimental data.

4.1.7. BA-TNO unobstructed tests

The BA-TNO experiments were conducted in the TNO "Pollution Industrial Aerodynamics" wind-tunnel facility (Nielsen & Ott, 1996). The test section of the wind tunnel is 6.8 m long, 2.65 m wide and 1.2 m high. The BA-TNO wind-tunnel tests were designed to a 1:78 scale and consisted of long duration, surface-level releases of SF_6. The gas was introduced through a 107 mm diameter orifice covered by a 50% porosity gauze to give a vertical low-momentum release. The gas concentration was measured at floor level using aspirated hot-wire probes.

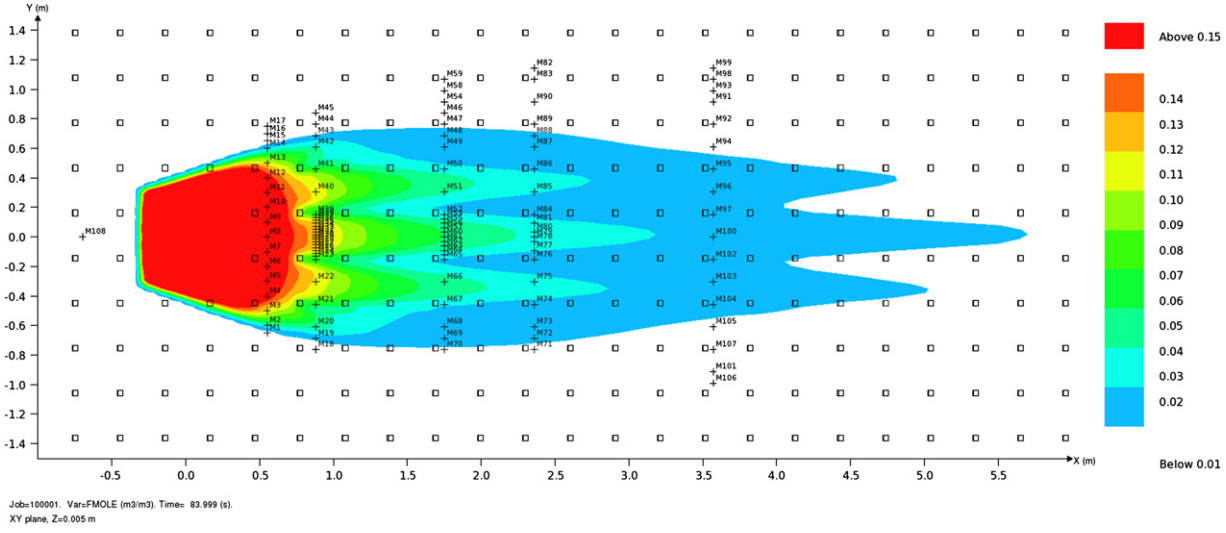

Fig. 15. Steady-state plume for test CHRC − A.

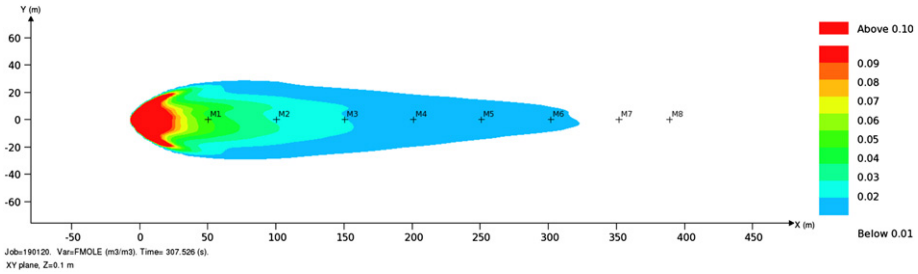

Fig. 17. Steady-state plume for test DAT0120.

The BA-TNO wind-tunnel experiments consisted of three cases, two of which (TUV01 and FLS) examined the unobstructed dispersion of the dense cloud, while the third test (TUV02) examined the effect of a barrier perpendicular to the wind direction and will therefore be discussed with the Group 2 tests.

The FLACS simulations were performed at "field" scale to comply with the FLACS meshing guidelines. The gas was introduced as a diffusive leak from a cylindrical hole of 8.35 m diameter covered by a disc with 50% vertical porosity. Terrain was assumed to be flat. A logarithmic wind profile was specified at the inlet boundary, with 10% turbulence intensity and turbulence length scale of 0.2 m. Sensors were assumed to be at ground level.

The computational domain for the TUV01 test stretched from −25 to 100 m in the wind direction, from −50 to 50 m in the crosswind direction and from −3 to 25 m elevation (the negative elevation was necessary to accommodate the gas leak volume); the grid size in the near field was 0.5 m × 0.5 m × 0.1 m, with a total of approximately 380,000 grid cells. The computational domain for the FLS test stretched from −80 to 350 m in the wind direction, from −75 to 75 m in the crosswind direction and from −3 to 25 m elevation; the grid size in the near field was 1 m × 1 m × 0.2 m, with a total of approximately 250,000 grid cells.

An example of the FLACS simulation is provided in Fig. 22, which shows the gas cloud (color-coded according to gas concentration by volume) at 0.1 m elevation for test TUV01. The figure also reports the peak gas concentrations measured during the test: it is counterintuitive and unclear to the authors how the unobstructed dispersion of a dense gas cloud, released at ground level with no vertical momentum, may result in higher concentrations (4.1%) farther downwind than closer to the source (1.4–1.8%), as the experimental data indicate. Regardless of this apparent inconsistency in the experimental data, the FLACS model predictions

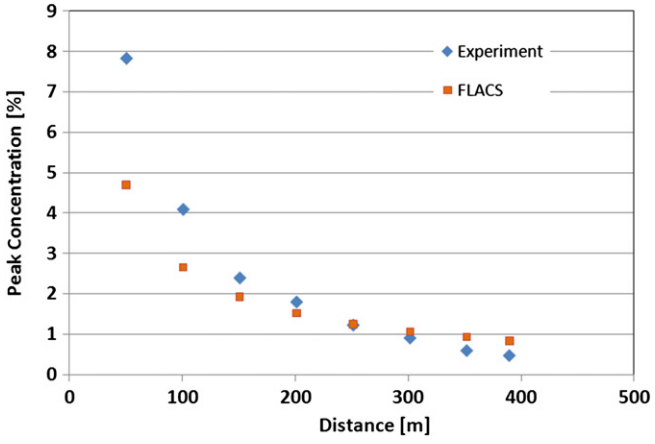

Fig. 18. Measured versus predicted concentrations for test DAT0120.

remain within approximately 1% (by volume) of the experimental measurements at all arcs included in the MVD, as shown in Fig. 23. Even better agreement with experimental data was obtained for the FLS test, as shown in Fig. 24.

4.2. Group 2: obstructed dispersion tests

4.2.1. CHRC tests B and C

As described earlier, CHRC tests B and C consisted of CO_2 releases (with propane added as a tracer gas) where the dispersion of the cloud was affected by obstructions: a tank and dike in test B, and a dike only in test C. Consistent with the 1:150 scaling of the wind tunnel, the dike was a square with an inner dimension of 63 cm and a wall height of 3.7 cm, while the tank was 31 cm in diameter with a spherical dome top and an overall height of 28.3 cm. The tank was located in the center of the dike. The gas was released through a meshed screen from the area inside the dike.

The FLACS simulations were performed at wind-tunnel scale, with the addition of the dike (and tank in test B) to the test A geometry. The same mesh, wind profile and gas leak characteristics were used as previously described for test A.

Fig. 25 shows the gas cloud iso-contours for test B (top) and C (bottom), and Fig. 26 shows the correlation between predicted and measured gas concentration at several locations for both tests. The model predictions fall within a "factor-of-2" of the experimental data at 100% of the measurement locations, with remarkable accuracy as the cloud disperses downwind. The model also correctly predicted the bifurcation of the cloud, due to the wake behind the storage tank, as it emerges from the diked area in test B (Fig. 25, top).

4.2.2. BA-Hamburg obstructed tests

As described earlier, several of the BA-Hamburg wind-tunnel tests examined the effect of fences on the dispersion of dense gas clouds. Different fence layouts were used for the various tests: a semicircular fence, either upwind or downwind of the release, or a circular fence. In all cases, the fence height was 3 cm, while the diameter was varied, being either 19 or 30 cm. It should be noted that the MVD description of some of these tests incorrectly indicates the diameter of the fence as equal to the distance from the source to the fence; the correct description should be that the distance is equal to the radius of the fence, as shown in the report by Nielsen and Ott (1996). As for the unobstructed tests, the experiments were at a model scale of 1:164, corresponding to a field-scale fence height of approximately 5 m. Gas concentration measurements were made at floor level using an aspirated hot-film probe.

The FLACS simulations were performed at field scale in order to comply with the FLACS meshing guidelines. The gas source was specified as a diffusive leak from a cylindrical hole of 11.2 m diameter, covered by a plate with 50% vertical porosity. The ground was assumed to be flat, with a 5 m tall fence and sensors were

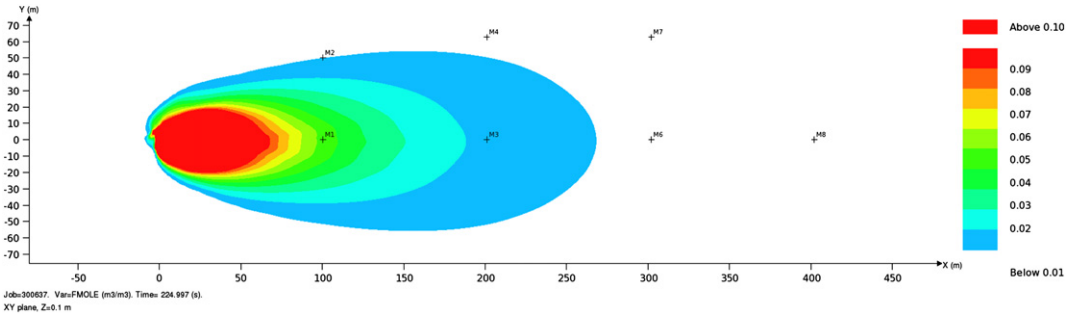

Fig. 19. Steady-state plume for test DAT637.

defined at ground level (5 cm elevation in field scale). A logarithmic wind profile was specified at the inlet boundary, with 5% turbulence intensity and turbulence length scale equal to the smallest grid cell size. The computational domain for vapor dispersion stretched from −80 to 250–480 m (depending on the test) in the wind direction, from −75 to 75 m in the crosswind direction and from −3 to 25 m elevation. The grid resolution in the near field was 1 m by 1 m by 0.2 m and stretched progressively away from the release. The total grid cell count was approximately 240,000.

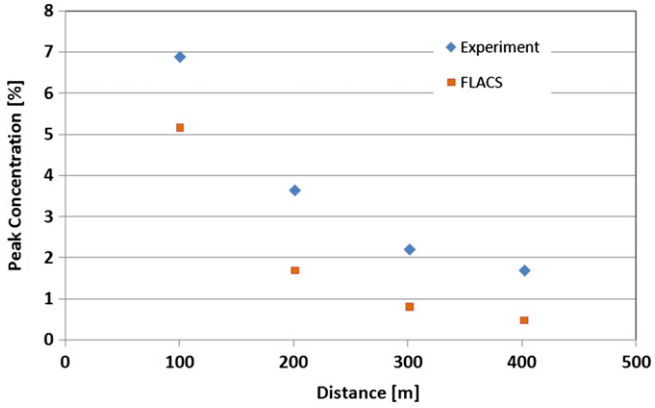

Fig. 20. Measured versus predicted concentrations for test DAT637.

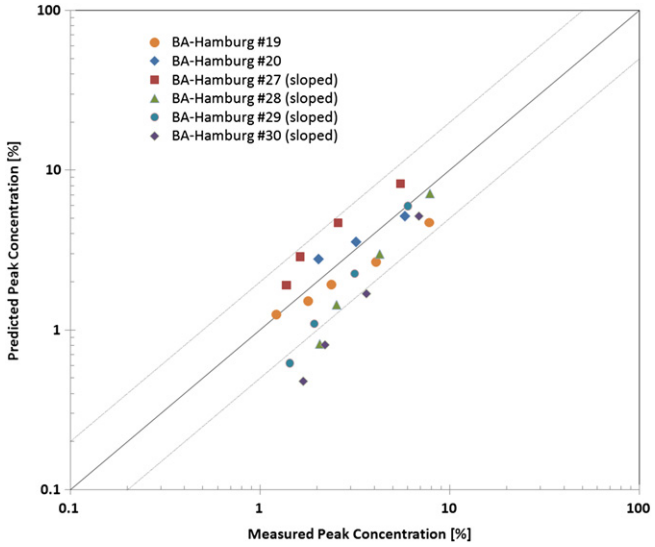

Fig. 21. Correlation of simulated to experimental gas concentration for the BA-Hamburg unobstructed tests.

The location of sensors for these tests was not clearly defined. In particular, it was not clear whether sensors were placed only along the axis of the wind tunnel or distributed crosswind at each arc location. The analysis of the simulation results suggested that there had to be multiple sensors at each arc to explain the experimental observations. Therefore, a set of sensors was specified in the FLACS model, at each arc location. For the semicircular fence tests, the maximum gas concentration at each arc was extracted for comparison with the experimental data. For the circular fence tests, instead, the average concentration at each arc was used to smooth out the effects of vortex shedding, consistent with the long averaging time of the aspirated probes.

An example of the FLACS simulation results is provided in Fig. 27, which shows the gas cloud at 0.8 m elevation (color-coded according to gas concentration by volume) for test DA0532 (semicircular fence located downwind of the release). For the same test, Fig. 28 compares the predicted and measured peak gas concentration at several distances from the spill location. The results show an excellent correlation between simulation and experimental results for this test. Similar results were obtained for the other BA-Hamburg obstructed tests included in the MEP database, as the correlation plot in Fig. 29 demonstrates: 97% of simulation results fall within the "factor-of-2" range with respect to the experimental data, with very good accuracy as the cloud reaches the farther sensors.

4.2.3. *BA-TNO obstructed test*

A single obstructed dispersion test from the BA-TNO series is included in the model validation database: test TUV02. This test

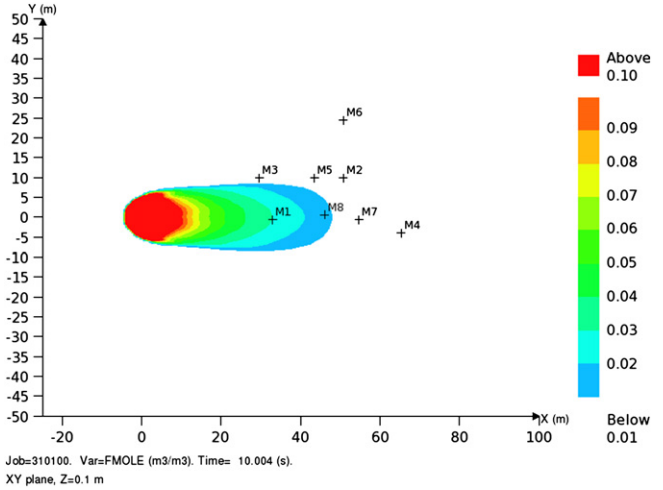

Fig. 22. Steady-state plume for test TUV01.

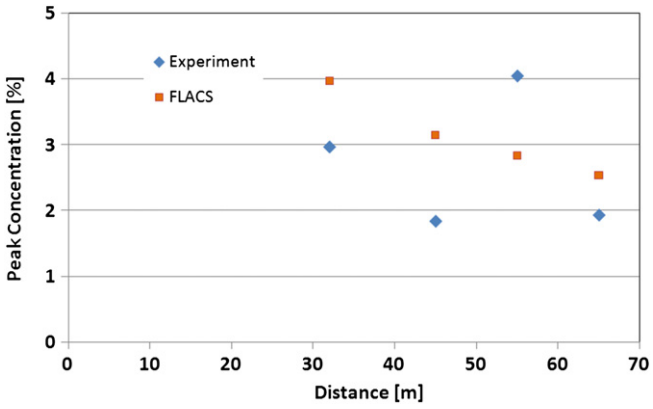

Fig. 23. Measured versus predicted concentrations for test TUV01.

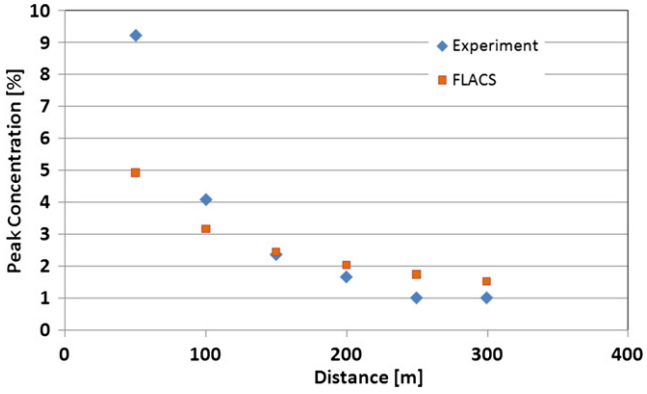

Fig. 24. Measured versus predicted concentrations for test FLS.

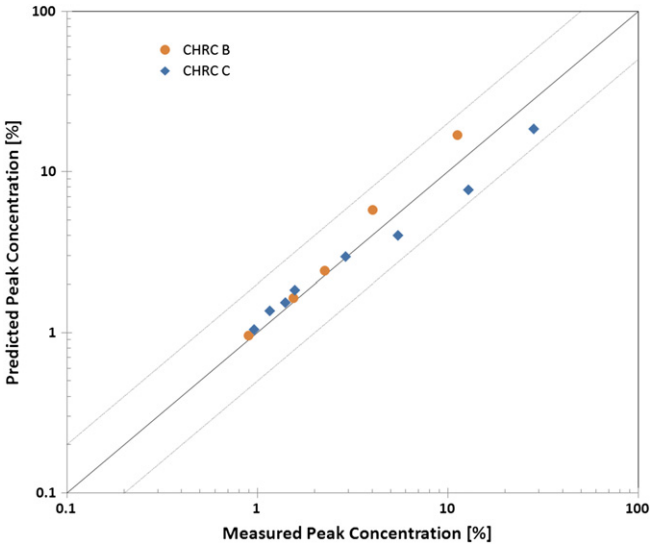

Fig. 26. Correlation of simulated to experimental gas concentration for the CHRC obstructed tests.

was similar to TUV01 (previously discussed) but with the addition of a linear fence perpendicular to the wind direction. The MVD provided no information about the length of the fence, however, based on the report by Nielsen and Ott (1996) it appears that the fence may have spanned the full width of the wind tunnel.

The FLACS simulations were performed at "field" scale to comply with the FLACS meshing guidelines. The gas was introduced as a diffusive leak from a cylindrical hole of 8.35 m diameter covered by a disk with 50% vertical porosity. Terrain was assumed to be flat. A logarithmic wind profile was specified at the inlet boundary, with 10% turbulence intensity and turbulence length scale of 0.2 m. Sensors were assumed to be at ground level.

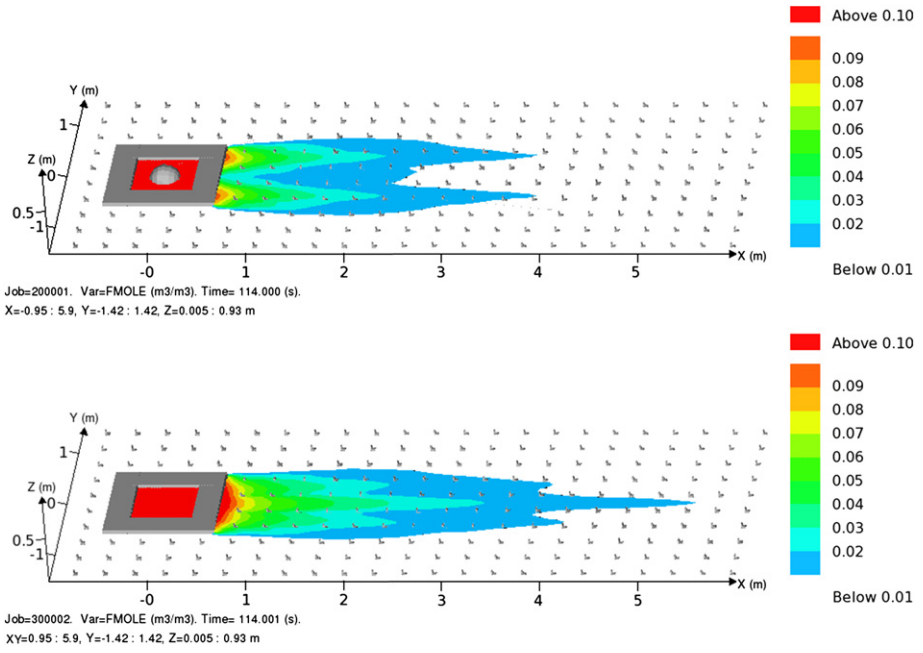

Fig. 25. FLACS simulations for tests CHRC Case B (top) and Case C (bottom).

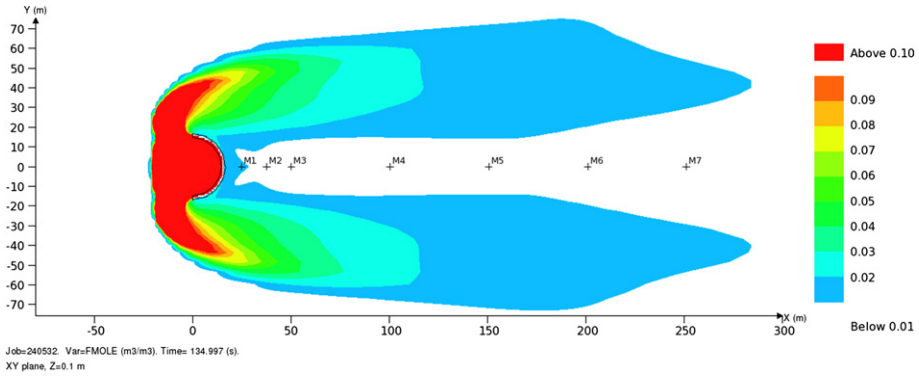

Fig. 27. Steady-state plume for test DA0532.

The computational domain for the TUV02 test stretched from −25 to 100 m in the wind direction, from −50 to 50 m in the crosswind direction and from −3 to 25 m elevation; the grid size in the near field was 0.5 m × 0.5 m × 0.1 m, for a total of approximately 380,000 grid cells.

An example of the FLACS simulation is provided in Fig. 30, which shows the gas cloud (color-coded according to gas concentration by volume) at 0.1 m elevation for test TUV02. The figure also reports the peak gas concentrations measured during the test: as for the TUV01 test, the pattern of concentrations in the reported experimental data is counterintuitive, as higher gas concentrations (4.4%) were measured downwind of the fence than upwind (2.0–2.5%). Regardless of this apparent inconsistency, the FLACS model predictions remain close to the experimental measurements at all other locations included in the MVD, as shown in Fig. 31.

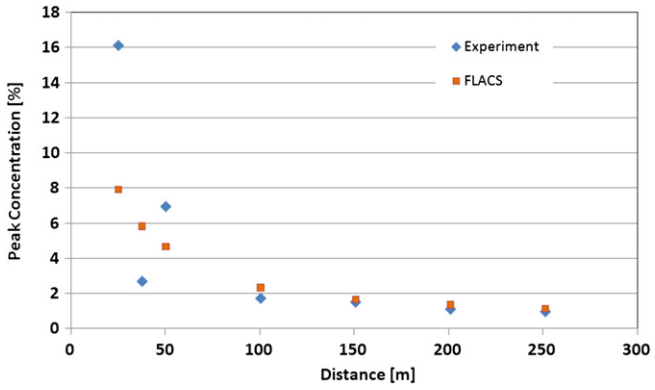

Fig. 28. Measured versus predicted concentrations for test DA0532.

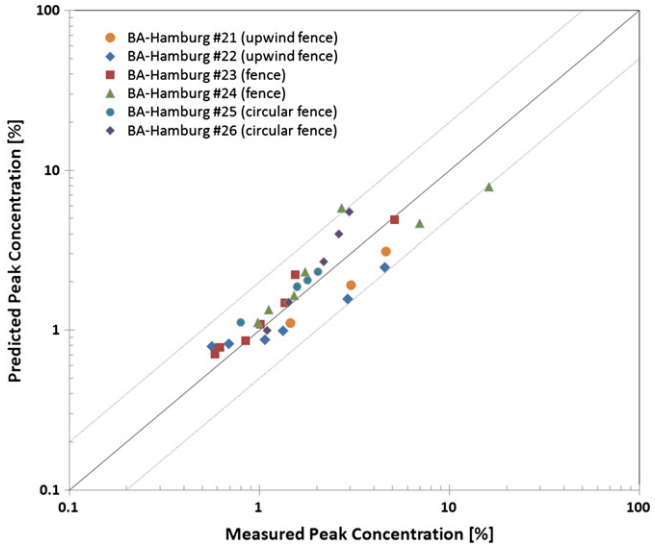

Fig. 29. Correlation of simulated to experimental gas concentration for the BA-Hamburg obstructed tests.

4.2.4. Falcon test series

The Falcon test series consisted of five large-scale LNG spill tests performed by the Lawrence Livermore National Laboratory in 1987 at Frenchman Flat, Nevada (Brown et al., 1990). The purpose of the tests was to evaluate the effectiveness of vapor fences as a mitigation technique for accidental LNG releases as well as to provide a data set for model validation purposes (see Fig. 32). For this reason, LNG was spilled onto a specially designed water pond equipped with a circulating system to maximize evaporation of the LNG pool.

LNG was delivered through a spill "spider" consisting of four pipes (each 11.6 m long) spaced at 90° intervals in order to distribute the LNG pool over the water pond. The ends of the spider arms pointed downward and were fitted with splash plates at the water surface, to prevent the LNG from sinking into the water.

Gas concentration and temperature sensors were mounted on towers distributed in three rows at 50 m, 150 m and 250 m from the fenced area. Each instrumentation tower had sensors at 1 m, 5 m, 11 m and 17 m above ground. The instrument array centerline was oriented at 225° to coincide with the prevailing wind direction.

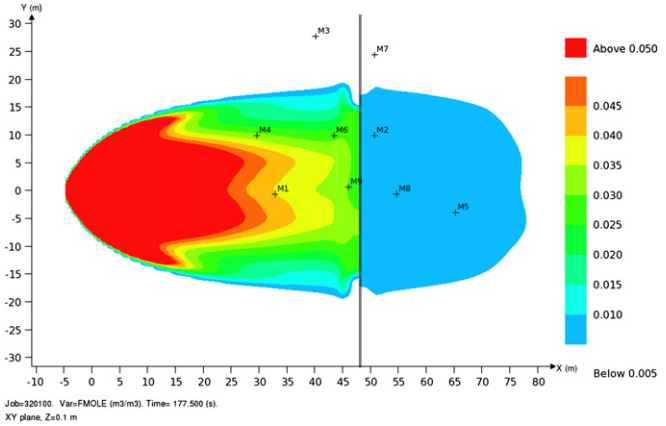

Fig. 30. FLACS simulations and experimental data for test TUV02.

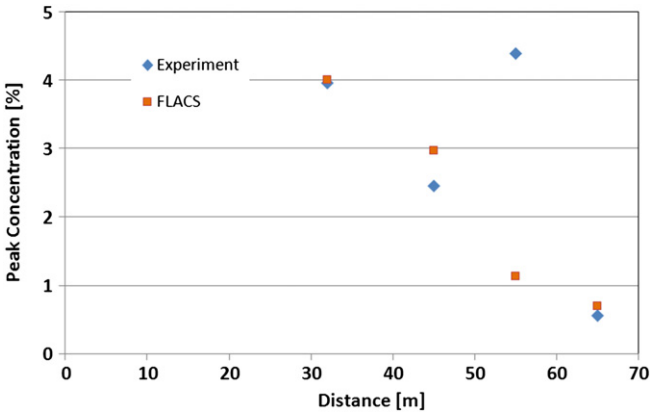

Fig. 31. Measured versus predicted concentrations for test TUV02.

Three tests were included in the Model Validation Database, as summarized in Table 8.

The FLACS pool model was used to calculate the spreading and vaporization of the LNG pool formed by the spill. The main geometry features, including the spill pond, vapor fences and wall were included in the model. The computational domain stretched from −150 to 300 m in the *x*-direction, from −100 to 100 m in the *y*-direction and from 0 to 50 m in elevation; the grid size in the near field was 1 m × 1 m × 0.25 m, for a total of approximately 500,000 grid cells.

An example of the FLACS simulation for the Falcon 1 test is provided in Fig. 33, which shows the gas cloud (at LFL concentration) approximately 60 s into the release. It can be observed how the flammable cloud is still almost entirely within the fenced area. In this case (as well as the other two Falcon tests) the gas concentrations predicted by FLACS at the first row of sensors (50 m downwind) largely underpredict the experimental results. This is most likely due the different way the LNG vapor source term was represented in the FLACS simulations versus the actual LNG spill mechanism in the experiments. As indicated above, the FLACS simulations used the pool model to calculate the LNG vapor generation from the spill, which was used successfully for all other large-scale LNG spill tests included in the model validation database. The main difference between the Falcon tests and the other LNG spill tests (Burro, Coyote and Maplin Sands) is the presence of the vapor fence surrounding the LNG spill pond. As Gavelli et al. pointed out (Gavelli, Bullister, & Kytomaa, 2008), when an LNG pool is exposed to ambient wind, the ambient turbulence tends to dominate over the turbulence associated with the LNG release and the pool boiling. In the Falcon tests, however, the tall vapor fence shields the LNG pool from the ambient wind; in this case, the characteristics of the LNG release control the growth of the vapor cloud within the fenced area.

Table 8
Falcon tests included in the MEP database.

Test no.	Wind speed (m/s)	Material	Release flow (kg/s)	Duration (s)
1	1.2	LNG	202	131
3	3.7	LNG	133	154
4	4.3	LNG	61	301

Based on a review of videos from the Falcon 5 test, the LNG release appears to be a high-pressure jet with associated flashing and aerosol formation. Therefore, a new simulation of the Falcon 1 test was performed, for evaluation purposes, using a new two-phase model that is being developed and that will allow FLACS to simulate the release and dispersion of high-pressure flashing jets. A snapshot of the vapor cloud (at LFL concentration) emerging from the fenced area is shown in Fig. 34. The new model shows a noticeable increase in the size of the flammable cloud overflowing the vapor fence, and the behavior of the visible cloud shows many similarities with videos from the Falcon 5 test. This is a significant improvement in the model prediction of the Falcon 1 test, which confirms the need for a physically accurate representation of the LNG vapor source term. These observations suggest that the pressurized LNG release for the Falcon experiments (and possibly for other field tests) may have been accompanied by flashing and aerosol formation and that neglecting the effect of these phenomena on the growth of the LNG vapor cloud may lead to significant prediction errors.

4.3. Assessment of FLACS with respect to the MEP acceptance criteria

The results of the FLACS simulations described in the previous sections can be grouped together in the following plots to allow an

Fig. 32. Falcon test setup — courtesy of R.P. Koopman.

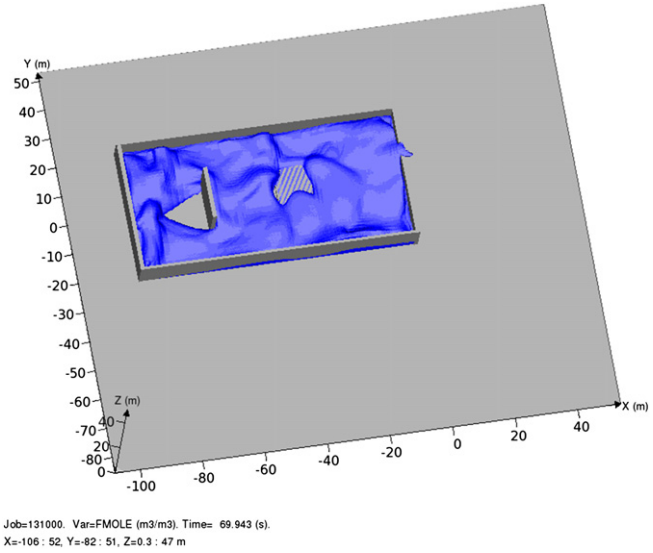

Fig. 33. LFL isosurface for the Falcon 1 LNG vapor cloud using the pool model, approximately 60 seconds into the release.

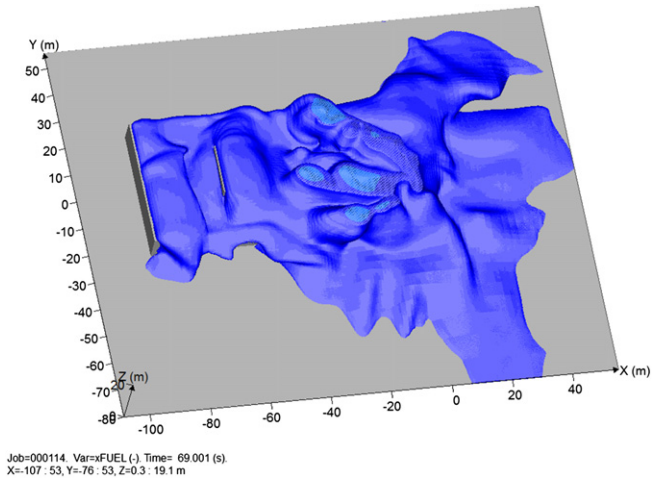

Fig. 34. LFL isosurface for the Falcon 1 LNG vapor cloud using the flashing jet release model, approximately 40 s into the test.

overall perspective on the performance of the model. Fig. 35 shows the correlation of predicted to experimental data for all 15 unobstructed tests in the MVD ("Group 1"), while Fig. 36 shows the same correlation for all 18 obstructed tests ("Group 2"). Within each Group, the comparison is performed separately for the field tests (left), for which short averaging times data is available, and wind-tunnel tests (right), for which only long averaging times data is reported.

A few observations can be drawn from these plots:

- The FLACS prediction of the unobstructed cloud dispersion tests is very good for both field and wind-tunnel tests. Overall, approximately 88% of data points from the Group 1 (unobstructed) tests fall within the "factor-of-2" range. As a term of comparison, Hanna et al. (2004) define a "good model" as one where at least 50% of data points fall within this range.
- The FLACS prediction of the wind-tunnel tests for obstructed cloud dispersion is also very good. A remarkable 98% of data points from the Group 2 wind-tunnel tests fall within the "factor-of-2" range.
- Only one set of tests is available to evaluate the obstructed cloud dispersion at field scale: the Falcon test series. As discussed previously, the FLACS pool model did not adequately represent the characteristics of the LNG release during the Falcon tests. The new two-phase jet release model being developed for FLACS, however, is showing great potential for a more realistic characterization of the LNG vapor source under those conditions. Based on the very good performance of the FLACS pool and dispersion models for all other tests in the

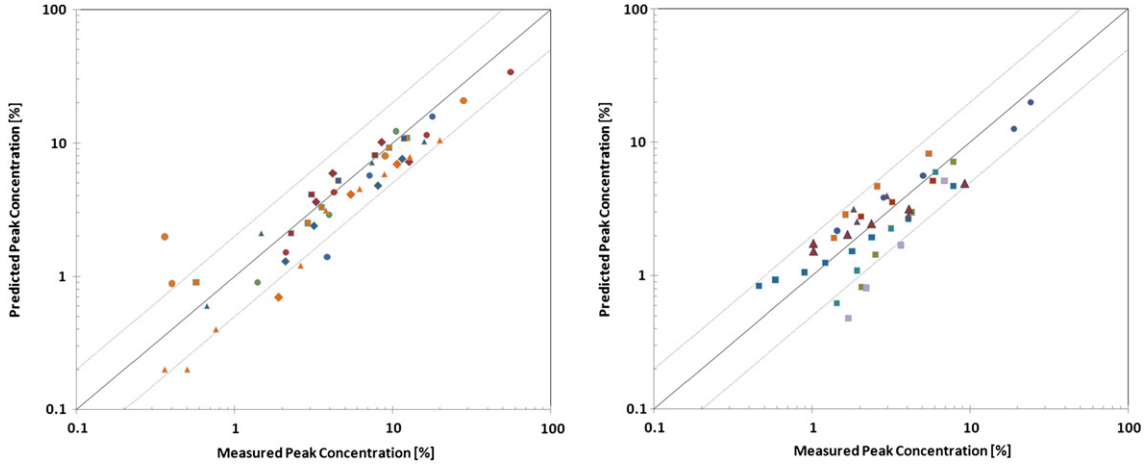

Fig. 35. Correlation of simulated to experimental gas concentration for unobstructed tests: field tests (left) and wind-tunnel test (right).

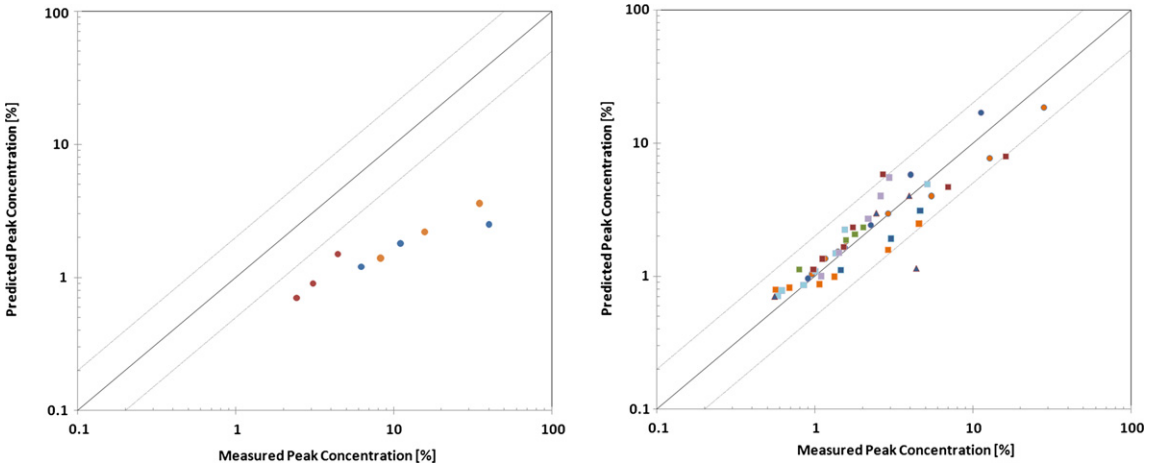

Fig. 36. Correlation of simulated to experimental gas concentration for obstructed tests: field tests (left) and wind-tunnel test (right).

Table 9
FLACS statistical performance parameters against the model validation database, using the "short" averaging times (i.e., field tests).

SPM	Results for Group 1 tests	Results for Group 2 tests (Falcon only)	Acceptability range
MRB	0.16	1.35	$-0.4 < \text{MRB} < 0.4$
MG	1.18	5.56	$0.67 < \text{MG} < 1.5$
MRSE	0.12	1.88	$\text{MRSE} < 2.3$
VG	1.14	23.65	$\text{VG} < 3.3$
FAC2	0.94	0.00	$0.5 < \text{FAC2}$

Table 10
FLACS statistical performance parameters against the model validation database, using the "long" averaging times (i.e., wind-tunnel tests).

SPM	Results for Group 1 tests	Results for Group 2 tests	Acceptability range
MRB	0.25	−0.02	$-0.4 < \text{MRB} < 0.4$
MG	1.34	0.98	$0.67 < \text{MG} < 1.5$
MRSE	0.29	0.07	$\text{MRSE} < 2.3$
VG	1.61	1.07	$\text{VG} < 3.3$
FAC2	0.89	0.98	$0.5 < \text{FAC2}$

MVD, it can be concluded that the problem with the Falcon tests is due to the inaccurate definition of the LNG release in the MVD, rather than to a deficiency with the model.

The MEP defines a set of statistical performance measures (SPM) that need to be calculated in order to provide a quantitative assessment of the capability of a model to "predict reality". Once the simulation results are entered in the workbook distributed with the *Guide to the LNG Model Validation Database* (Coldrick et al., 2009), the performance parameters are automatically calculated. For each model, the SPMs are to be calculated separately for the Group 1 (unobstructed dispersion) and Group 2 (obstructed dispersion) tests, as well as for "short" and "long" averaging times (respectively, field tests and wind-tunnel tests, as discussed previously). The SPM results from the FLACS simulations for Group 1 and Group 2 are shown in Tables 9 and 10, respectively, for the short and long averaging times. It should be noted that the Group 2 column in Table 9 includes only the Falcon test series, for which the inadequate source term definition by the MVD has already been discussed in this paper. All other statistical performance parameters fall within their respective acceptability ranges.

Based on the results shown in the SPM tables above, it can be concluded that FLACS successfully meets the quantitative criteria for LNG vapor dispersion model validation as established in the MEP. The validation effort was also valuable in helping the authors identify areas for further improvement of the model, such as: improved handling of terrain features, more accurate representation of fluctuating wind boundary conditions, and completion of the two-phase flashing jet release model for a more physically realistic representation of complex releases such as in the Falcon test series.

5. Conclusions

GexCon's CFD software FLACS was used to simulate the full set of tests in the model validation database of the *model evaluation protocol for LNG vapor dispersion* (MEP). The stated purpose of the MEP is to "provide a comprehensive methodology for determining the suitability of models to accurately simulate the dispersion of vapors emanating from accidental spills of LNG on land". In order to do so, it provides experimental results from a set of 33 field-scale and wind-tunnel tests, and specifies a set of quantitative statistical performance measures that should be met by a model in order to be considered suitable for LNG vapor dispersion modeling.

The result of the model validation effort described in this paper is that FLACS met or exceeded the statistical performance measures for all groups of tests (that is, unobstructed or obstructed dispersion, and field or wind-tunnel scale), with the noted exception of the Falcon test series, whose peculiar LNG release conditions have been identified as the reason for the model's underprediction of the experimental results. Therefore, FLACS can be considered a suitable model to accurately simulate the dispersion of vapor from an LNG spill.

References

van den Bosch, C. J. H., & Weterings, R. A. P. M. (1997). Methods for the calculation of physical effects due to the release of hazardous materials (liquids and gases). CPR14E *TNO yellow book* (3rd ed.). The Hague, The Netherlands: TNO.

Brown, T. C., Cederwall, R. T., Chan, S. T., Ermak, D. L., Koopman, R. P., Lamson, K. C., et al. (June 1990). *Falcon series data report: 1987 LNG vapor barrier verification field*. Report no. GRI-89/0138. Gas Research Institute. http://www.osti.gov/bridge/servlets/purl/6633087-9HP88a/.

Carissimo, B., Jagger, S. F., Daish, N. C., Halford, A., Selmer-Olsen, S., Riikonen, K., et al. (2001). The SMEDIS database and validation exercise. *International Journal of Environment and Pollution, 16*(1–6), 614–629.

Coldrick, S., Lea, C. J., & Ivings, M. J. (24th February 2009). *Validation database for evaluating vapor dispersion models for safety analysis of LNG facilities, guide to the LNG model validation database*. The Fire Protection Research Foundation. http://www.nfpa.org/assets/files/PDF/Research/LNG_database_guide.pdf.

Colenbrander, G. W., Evans, A., & Puttock, J. S. (May 1984a). Spill tests of LNG and refrigerated liquid propane on the sea *Maplin Sands 1980: Dispersion data digest; trial 27*. Shell Research Ltd, Thornton Research Centre. Report TNER.84.028.

Colenbrander, G. W., Evans, A., & Puttock, J. S. (May 1984b). Spill tests of LNG and refrigerated liquid propane on the sea *Maplin Sands 1980: Dispersion data digest; trial 34*. Shell Research Ltd, Thornton Research Centre. Report TNER.84.030.

Colenbrander, G. W., Evans, A., & Puttock, J. S. (May 1984c). Spill tests of LNG and refrigerated liquid propane on the sea *Maplin Sands 1980: Dispersion data digest; trial 35*. Shell Research Ltd, Thornton Research Centre. Report TNER.84.031.

Dharmavaram, S., Hanna, S. R., & Hansen, O. R. (2005). Consequence analysis – using a CFD model for industrial sites. *Process Safety Progress, 24*, 316–327.

Ermak, D. L., Chapman, R., Goldwire, H. C., Jr., Gouveia, F. J., & Rodean, H. C. (October 1988). *Heavy gas dispersion test summary report*. UCRL-21210. Lawrence Livermore National Laboratory.

FLACS v9.1 user's manual. (2009).

Flaherty, J. E., Allwine, K. J., Brown, M. J., Coirier, W. J., Ericson, S. C., Hansen, O. R. et al. (2007). Evaluation study of building-resolved urban dispersion models. In *Seventh symposium on the urban environment*, 10–13 September 2007.

Gavelli, F., Bullister, E., & Kytomaa, H. (2008). Application of CFD (Fluent) to LNG spills into geometrically complex environments. *Journal of Hazardous Materials, 159*, 158–168.

Goldwire, H. C., Jr., Rodean, H. C., Cederwall, R. T., Kansa, E. J., Koopman, R. P., McClure, J. W., et al. (1983). UCID-19953*Coyote series data report: LLNL/NWC 1981 LNG spill tests dispersion, vapor burn and rapid-phase transitions, Vols. 1–2*. Lawrence Livermore National Laboratory. https://e-reports-ext.llnl.gov/pdf/195030.pdf and https://e-reports-ext.llnl.gov/pdf/195363.pdf.

Han, J., Arya, S. P., Shen, S., & Lin, Y. L. (2000). *An estimation of turbulent kinetic energy and energy dissipation rate based on atmospheric boundary similarity theory*. Tech. Rep. CR-2000-210298. USA: NASA.

Hanna, S. R., Chang, J. C., & Strimaitis, D. G. (1993). Hazardous gas model evaluation with field observations. *Atmospheric Environment, 27 A*(15), 2265–2285.

Hanna, S. R., Hansen, O. R., & Dharmavaram, S. (2004). FLACS CFD air quality model performance evaluation with Kit Fox, MUST, Prairie Grass and EMU observations. *Atmospheric Environment, 38*, 4675–4687.

Hanna, S. R., Hansen, O. R., Ichard, M., & Strimaitis, D. (2009). Computational fluid dynamics (CFD) model simulations of dispersion from chlorine railcar releases in industrial and urban areas. *Atmospheric Environment, 43*, 262–270.

Hanna, S. R., Strimaitis, D. G., & Chang, J. C. (1991). *Evaluation of commonly-used hazardous gas dispersion models*. In *Hazard response modelling uncertainty (a quantitative method), Vol. II*. Sigma Research Corporation. Final report; April 1989–April 1991.

Hansen, O. R., Melheim, J. A., & Storvik, I. E., 2007. CFD-modeling of LNG dispersion experiments. In *AIChE Spring national meeting, 7th topical conference on natural gas utilization*, Houston, USA.

Havens, J., & Spicer, T. (2005). LNG vapor cloud exclusion zones for spills into impoundments. *Process Safety Progress, 24*(3), 181–186.

Havens, J., & Spicer, T. (October 2006). *Vapor dispersion and thermal hazard modelling*. Final topical report to Gas Technology Institute under sub-contract K100029184.

Havens, J., Spicer, T., & Sheppard, W. (2007). Wind tunnel studies of LNG vapor dispersion from impoundments. In *AIChE national Spring meeting*, Houston.

Hjertager, B. H. (1986). Three-dimensional modeling of flow, heat transfer, and combustion (pp. 304–350) *Handbook of heat and mass transfer*. P.O. Box 2608, Houston, Texas 770011: Gulf Publishing Company.

Incopera, F. P., & de Witt, D. P. (1996). *Fundamentals of heat and mass transfer*. Wiley Ed.

Ivings, M. J., Jagger, S. F., Lea, C. J., & Webber, D. M. (May 9, 2007). *Evaluating vapor dispersion models for safety analysis of LNG facilities*. The Fire Protection Research Foundation. http://www.nfpa.org/assets/files/PDF/Research/LNGVaporDispersionModel.pdf.

Koopman, R. P., Baker, J., Cederwall, R. T., Goldwire, H. C., Jr., Hogan, W. J., Kamppinen, L. M., et al. (1982). UCID-19075 *Burro series data report LLNL/NWC 1980 LNG spill tests, Vols. 1–2*. Lawrence Livermore National Laboratory. https://e-reports-ext.llnl.gov/pdf/194414.pdf and https://e-reportsext.llnl.gov/pdf/194606.pdf.

Koopman, R. P., Cederwall, R. T., Ermak, D. L., Goldwire, H. C., Jr., Hogan, W. J., McClure, J. W., et al. (1982). Analysis of Burro series 40 m^3 LNG spill experiments. *Journal of Hazardous Materials, 6*, 43–83.

Launder, B. E., & Spalding, D. B. (1974). The numerical computation of turbulent flows. *Computer Methods in Applied Mechanics and Engineering, 3*, 269–289.

McQuaid, J. (Ed.). (1987). Heavy gas dispersion trials at Thorney Island – 2. In *Proceedings of a symposium held at the University of Sheffield*, Great Britain, September 1986. *Journal of Hazardous Materials, 16*, 1–502.

Middha, P., Hansen, O. R., Grune, J., & Kotchourko, A. (2010). CFD calculations of gas leak dispersion and subsequent gas explosions: validation against ignited impinging hydrogen jets. *Journal of Hazardous Materials, 179*, 84–94.

Model Evaluation Group. (1994). Guidelines for model developers. European Communities Directorate General XII Science Research and Development.

Model Evaluation Group. (1994). Model evaluation protocol. European Communities Directorate General XII Science Research and Development.

Nielsen, M., & Ott, S. (March 1996). *A collection of data from dense gas experiments*. Riso-R-845 (EN). Denmark: Riso National Laboratory. http://www.risoe.dtu.dk/research/sustainable_energy/energy_systems/projects/rediphem.aspx.

Puttock, J. S., Blackmore, D. R., & Colenbrander, G. W. (1982). Field experiments on dense gas dispersion. *Journal of Hazardous Materials, 6*, 13–41.

Rohsenow, W. M. (1952). A method of correlating heat transfer data for surface boiling of liquids. *Transactions of the ASME, 74*, 969–976.